UNIVERSITY OF CALIFORNIA SAN DIEGO

Ubiquitylation of Histone Octamers by the ASB9-CUL5 E3 Ligase

A Thesis submitted in partial satisfaction of the requirements for the degree Master of Science

in

Chemistry

by

Christopher Joseph Condon

Committee in charge:

Professor Elizabeth Komives, Chair
Professor Rommie Amaro
Professor Galia Debelouchina

2018

The Thesis of Christopher Joseph Condon is approved, and it is acceptable in quality and form for publication on microfilm and electronically:

_____

_____

_____

Chair

University of California San Diego

2018

TABLE OF CONTENTS

LIST OF ABBREVIATIONS

Å	Angstrom
ACN	Acetonitrile
AE	ASB9-ElonginsB/C
AECR	ASB9-ElonginsB/C-Cullin 5- Rbx2
AMP	Ampicillin
CAM	Chloramphenicol
CK	Creatine Kinase
CKB	Creatine Kinase B
CRL	Cullin-RING ligase
CUL5	Cullin 5
ECR	ElonginsB/C-Cullin 5-Rbx2
EloBC	Elongins B/C
EDTA	Ethylenediaminetetraacetic Acid
HDXMS	Hydrogen-Deuterium Exchange Mass Spectrometry
KAN	Kanamycin
LC-MS/MS	Liquid Chromatography-Tandem Mass Spectrometry
N8	Nedd8
PDB	Protein Data Bank
Rbx2	RING box protein 2
RING	Really Interesting New Gene

SDS-PAGE	Sodium Dodecyl Sulfate-Polyacrylamide Gel Electrophoresis
Ub	Ubiquitin

LIST OF FIGURES

LIST OF TABLES

ACKNOWLEDGEMENTS

I would like to acknowledge Professor Elizabeth Komives for her support as the chair of my committee. She provided me a space in her lab for me to hone my skills as a researcher and contribute my work to the field of Biochemistry. She has provided invaluable guidance throughout my research experience and Thesis preparation.

I would also like to acknowledge my mentor, Ryan Lumpkin, who has provided me invaluable guidance throughout my research project. He was the mastermind behind the purification of the CUL5-ASB9 ligase and always provided me with insightful advice through every step of my project.

I would also like to thank Dominic Narang, a fellow member of the Komives lab who provided me with and taught me how to prepare various proteins for my project. Many hours of life have been saved thanks to him. I would also like to acknowledge all the members of the Komives lab past and present who were there for me while I completed my Thesis research. They were always there for me when I needed advice, whether it was research or non-research related.

Lastly, I want to thank my family who have provided me with food, shelter and emotional support throughout my Thesis. I would not have made it without them.

Chapter II, in full, is currently being prepared for submission for publication of the material. Lumpkin, Ryan J.; Condon, Christopher J. The thesis author significantly contributed to this work as a researcher and author.

ABSTRACT OF THE THESIS

Ubiquitylation of Histone Octamers by the CUL5-ASB9 E3 Ligase

by

Christopher Joseph Condon

Master of Science in Chemistry

University of California San Diego, 2018

Professor Elizabeth A. Komives, Chair

Eukaryotic organisms have evolved to recycle proteins in process called Ubiquitylation. Attachment of ubiquitin molecules to a substrate protein act as a signal for the substrate protein to be degraded. The last step of ubiquitylation typically requires an enzyme called the E3 ubiquitin ligase. This work investigates the interactions between the CUL5-ASB9 E3 ligase and a novel substrate, histone octamers, through Hydrogen-Deuterium exchange and MALDI-TOF mass spectrometry.

Chapter II explains the *in vitro* expression and purification of the CUL5-ASB9 E3 ligase (AECR). There are many components to AECR which are not very soluble if purified separately. The purification strategy of co-expression in *E. coli* and co-purification of AECR showed to be successful. Additionally, we show AECR is active a capable of ubiquitylating histone octamers through *in vitro* activity assays and SDS-PAGE analysis.

Chapter III quantitatively confirms and characterizes the activity of AECR through liquid chromatography-tandem mass spectrometry (LC-MS/MS). We further confirm through mutagenesis of AECR and *in vitro* assays that AECR's histone ubiquitylation activity is not dependent on the modification called neddylation.

Chapter IV investigates the interactions between histones and ASB9, which is known to be the substrate receptor for AECR. Here we use Hydrogen-Deuterium exchange to identify changes in ASB9 upon histone binding. We observe that ASB9 increases in exchange when histones are present, but there is a small region of protection that may indicate the position where histones bind.

Chapter I

Introduction

A. Mechanism of Ubiquitylation

Eukaryotic organisms have evolved over time to utilize hundreds of different cell types, expressed at different times and locations in the body. These processes require precise control over gene expression, protein synthesis and regulation, all of which require a complex network of signals that include transcription factors and post-translational modifications(PTMs) of proteins. Among this signaling network, the PTM ubiquitylation stands as a key component of cellular function and is responsible for degradation, localization and interactions of thousands of proteins in the proteome. Ubiquitylation was initially recognized as an ATP-dependent process in the cell which involved proteolysis (*1*). Today, the biochemical mechanism of ubiquitylation has been studied extensively. In the first step of ubiquitylation, the ubiquitin molecule is activated via the E1 ubiquitin-activating enzyme which binds the ubiquitin molecule and ATP. E1 covalently attaches to the ubiquitin molecule by catalyzing a C-terminal acyl-adenylation reaction. Next, a catalytic cysteine in the E1 enzyme attacks the Ubiquitin-AMP intermediate through an acyl substitution, creating a thioester bond with ubiquitin and releasing an AMP (*2*). The activated E1-ubiquitin complex then transfers its ubiquitin to a catalytic cysteine on the E2 ubiquitin-conjugating enzyme in a trans-thioesterification reaction (*3*). Finally, the ubiquitin E3 ligase brings together the Ub-E2 and substrate molecules, catalyzing an isopeptide bond between a substrate lysine and the C-terminal glycine of Ubiquitin (*2*). The E3 ligase can repeat this reaction with the substrate, forming various polyubiquitin chains. The fate of a ubiquitylated substrate depends largely on its pattern of ubiquitylation. Monoubiquitylation can act as a signal in processes such as membrane trafficking and endocytosis (*4*). Substrates can be multi-monoubiquitylated as well, where multiple sites on the substrate are monoubiquitylated.

Polyubiquitylation is the formation of polyubiquitin chains where the C-terminal glycine of ubiquitin is linked to a lysine located on an adjacent ubiquitin molecule. Different lysine-linked polyubiquitin chains affect the cellular process the substrate will undergo. Ubiquitin molecules can be linked in different patterns depending on which lysine of the previous Ubiquitin is linked to the c-terminal glycine of the next. K48-linked polyubiquitylation is commonly associated with proteasomal degradation, where proteins are denatured and hydrolyzed into peptides inside the proteasome (*5*).

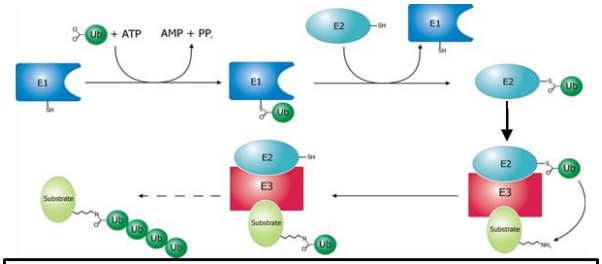

Figure 1.1: Schematic Diagram of the ubiquitylation cascade. This shows the role of the E1, E2, and E3 proteins as well as the chemical linkages between each protein and Ub (Figure adapted from Rogerdodd at the English language Wikipedia, CC BY-SA 3.0.

Ubiquitin acts as more than just a signal for proteasomal degradation, affecting many cellular processes like mitosis, inflammatory response and DNA-damage response. One of the more famous E3 ligases is the Anaphase Promoting Complex/Cyclosome (APC/C) which was discovered to signal degradation of anaphase inhibitors and allow sister chromatid separation during mitosis (*6*). Chromatin architecture can be changed by PTMs which determine transcription factor accessibility to gene sequences. The Polycomb repressive complex 1 (PRC1) is a regulator of histone ubiquitylation, which monoubiquitylates histone H2A and promotes chromatin compaction (*7*). In this case, ubiquitin acts additionally as a signal for the PRC2 complex which trimethylates H3 resulting in further chromatin condensation (*8, 9*). Ubiquitylation also plays an important role in inflammatory pathways such as NF-kB where

inhibitors of NF-kB, known as IkBs, are phosphorylated and consequently polyubiquitylated by an E3 ligase which targets it for degradation by the 26S proteasome (*10*). The ubiquitylation pathway plays a large role in many cellular processes, including many diseases. Thus, it has become a large field of research to discover and characterize the enzymes involved, especially E3 ligases and their substrates.

B. Cullin-RING E3 Ligases

In the human genome there are two E1 enzymes, 37 E2 enzymes, and over 600 E3 ubiquitin ligases (*11*). The high diversity of E3 ligases is due to their modular structure which grants many different combinations, each possessing different substrate specificities. The Cullin-RING-ligase(CRL) family makes up the largest class of E3 ligases in the human genome. CRLs regulate a massive amount of cellular processes in the body, from DNA replication to circadian rhythms and cell differentiation (*12, 13*). Despite their variety of regulatory functions, CRLs share a common structure with the most common feature being the cullin scaffold. There are 7 different cullins(CUL1-3, 4A, 4B, 5, 7) in the human genome that each serve as a scaffold for the multi-subunit complex. Cullins are known to be rigid molecules, containing an N-terminal stock composed of 3 five-helix bundles known as cullin repeats, and a C-terminal globular domain (*14*). The C-terminal side of each cullin contains a sequence that recruits the zinc-binding RING-H2 domain protein RBX1 or RBX2, which then recruits the Ub-E2 enzyme to the E3 ligase (*15, 16*). The N-terminus of each cullin contains a variable sequence which binds a different adaptor protein. Similarly, each adaptor protein contains a binding motif for many different substrate receptors (*17-19*). SKP1, the adaptor for Cul1, contains an F-Box motif that recruits specific substrate receptors (*18*), whereas Cul2 and Cul5 recruit the adaptors Elongins B & C which

contain a SOCS-box motif (*19*). Cul4A, 4B and 7 all similarly contain their own specific adaptor proteins and substrate receptors (*20*).

In addition to sharing structural similarities, CRLs also share a mechanism of regulation called Neddylation where the Ubiquitin-like molecule(UBL) NEDD8 is covalently attached to a single lysine on the cullin subunit (*21*). Neddylation requires its own NEDD8-activating E1(NAE1) and NEDD8 conjugating E2(UBE2F) enzymes which result in a similar isopeptide bond between the cullin lysine and C-terminal glycine of NEDD8 (*22*). In vitro studies have shown neddylation enhances CuL1 ligase dependent activity (*23*). Other CRLs have shown similar responses to neddylation, therefore it is thought neddylation plays an important role in regulating CRL ligase activity (*24*).

Despite their overwhelming abundance in cellular processes, the mechanism for Ubiquitin transfer by CRLs is still unknown. In addition, little structural information exists for most CRLs. The most well-characterized CRL is the CUL1 ligase(SCF), which there exists multiple crystal structures (*14, 25*). Based on the understood structure of SCF and the structural homology among CRLs, it can be extrapolated that CRLs share a similar macromolecular structure. In the final CRL-ligase complex, the substrate receptor along with its bound substrate are situated at the N-terminus of the cullin scaffold, whereas the RING containing E2 receptor and its corresponding E2 are located 50-60 angstroms away at the C-terminus of the cullin scaffold (*26, 27*). Such large distance between E2-Ub and the substrate raises the question of how E2 and substrate come into contact.

C. Cullin 5 and the ASB Receptor Family

The relevant CRL studied in this thesis is the CUL5-RING ligase. Cullin 5(CUL5) acts as the scaffold for the CUL5-RING ligase which exists in several conformational states tuned

through the addition of Nedd8 (*28, 29*). CUL5 localizes to the cell during cell division and to the cell membrane at the completion of cytokinesis which suggests it serves a role in cell division (*30*). CUL5 interacts with Rbx2 at its C-terminus and Elongins B and C at its N-terminus, forming a complex suitable for binding of E2 enzymes and different substrate receptors (*31, 32*). As of this date, no crystal structure of a complete Cul5 E3 ligase exists.

One of the larger family of substrate receptors for CUL5 is the Ankyrin repeat and SOCS box (ASB) family of proteins. ASBs are also a member of the suppressor of cytokine signaling (SOCS) superfamily and are associate most often with ECS-type (ElonginBC-Cullin-SOCS-box) CRL ligases. The SOCS box motif located at the C-terminal, is shared by almost all Cul5 E3 ligase substrate receptors and consists of a Cul5 box and a BC box which interact with CUL5 and Elongins B/C respectively (*32, 33*).

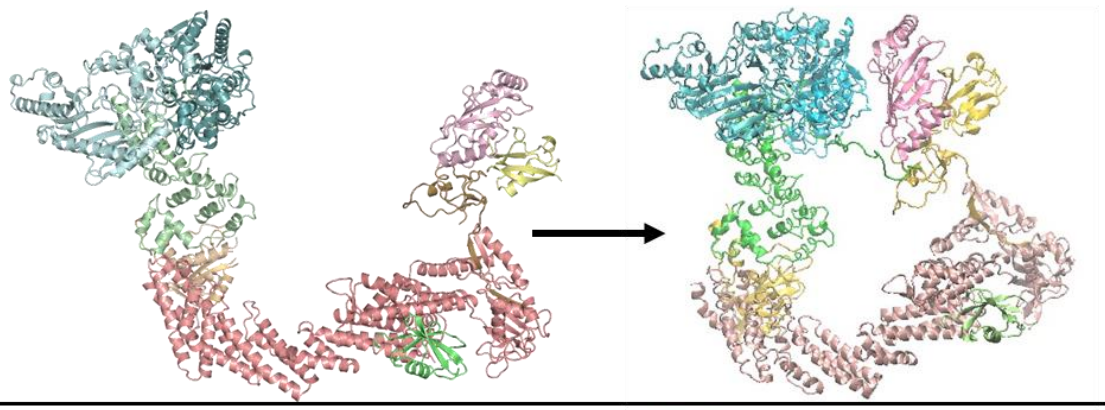

Figure 1.2: Model of the ASB9-CRL showing (from left to right) CK/CK dimer (42 kD, PBDs 3DRB, 3B6R) in pale cyan/light teal, ASB9 in pale green (32 kD, PDB 3ZKJ), EloB/C in wheat/light orange (17, 14 kD, PDB 3ZKJ), CUL5 in salmon (90kD, PDBs 2WZK, 1LDK: CUL1), RBX2 in sand (13 kD, PDB 4AP4: RNF4, UBE2, Ub), E2 in light pink (17 kD, PDB 4AP4: RNF4), Ub in yellow orange (8kD, 4AP4) and Nedd8 in limon. The open model was constructed from a combination of molecular docking (CKB on ASB9), partial structures (CUL5), and homology modeling (RBX2, UBE2D2). The closed model corresponds to the lowest normal mode of motion of the open model.

The quaternary structure of ASB9, Elongins B and C, and CUL5 have recently characterized (*34*)and the crystal structure of ASB9 with Elongins B and C also exist (*35, 36*). However, the ASB protein's association with its substrate remains poorly understood. ASB9 is well-studied member of the ASB family and has been shown to polyubiquitylate Creatine Kinase

(CK) (*37*). Crystal structures and biophysical studies show the interaction between ASB9 and CK, suggesting that ASB9 binds tightly to a dimer of CK and residues 1-252 of ASB9 place itself inside one CK active site (*35, 38*). Although ASB9-CK interaction has been characterized, there is little known about ASB9's interaction with other potential substrates. There is also no clear indication between how substrates bind to ASB9 and the substrate's pattern of ubiquitylation. There is no established method to construct the ASB9-CUL5 E3 ligase in vitro, so limited information exist regarding ubiquitylation activity and the regulatory effects of neddylation on substrate ubiquitylation.

D. References

1. Ciehanover, A., Hod, Y., and Hershko, A. (1978) A heat-stable polypeptide component of an ATP-dependent proteolytic system from reticulocytes, *Biochemical and Biophysical Research Communications 425*, 565–570.

2. Pickart, C. M. (2001) Mechanisms underlying ubiquitination *Annu Rev Biochem 70*, 503–533.

3. van Wijk, S. J., and Timmers, H. T. (2010) The family of ubiquitin-conjugating enzymes (E2s): deciding between life and death of proteins, *FASEB Journal 24*, 981–993.

4. Miranda, M., and Sorkin, A. (2007) Regulation of receptors and transporters by ubiquitination: new insights into surprisingly similar mechanisms, *Molecular Interventions. 7*, 157–167.

5. Komander, D. (2009) The emerging complexity of protein ubiquitination, *Biochem Soc Trans 37*, 937–953.

6. King, R. W., Peters, J. M., Tugendreich, S., Rolfe, M., Hieter, P., and Kirschner, M. W. (1995) A 20S complex containing CDC27 and CDC16 catalyzes the mitosis-specific conjugation of ubiquitin to cyclin B., *Cell. 81*, 279-288.

7. Wang, H., Wang, L., Erdjument-Bromage, H., Vidal, M., Tempst, P., Jones, R. S., and Zhang, Y. (2004) Role of histone H2A ubiquitination in Polycomb silencing., *Nature. 431*, 873-878.

8. Kalb, R., Latwiel, S., Baymaz, H. I., Jansen, P. W., Müller, C. W., Vermeulen, M., and Müller, J. (2014) Histone H2A monoubiquitination promotes histone H3 methylation in Polycomb repression., *Nat. Struct. Mol. Biol. 21*, 569–571.

9. Blackledge, N. P., Farcas, A. M., Kondo, T., King, H. W., McGouran, J. F., Hanssen, L. L., Ito, S., Cooper, S., Kondo, K., Koseki, Y., Ishikura, T., H.K., L., Sheahan, T. W., Brockdorff, N., Kessler, B. M., Koseki, H., and Klose, R. J. (2014) Variant PRC1 complex-dependent H2A ubiquitylation drives PRC2 recruitment and polycomb domain formation., *Cell. 157*, 1445-1459.

10. Miyamoto, S., Chiao, P. J., and Verma, I. M. (1994) Enhanced I kappa B alpha degradation is responsible for constitutive NF-kappa B activity in mature murine B-cell lines., *Mol Cell Biol 14*, 3276-3282.

11. Hershko, A., and Ciechanover, A. (1998) The ubiquitin system, *Annu Rev Biochem 67*, 425–479.

12. Deshaies, R. J., and Joazeiro, C. A. (2009) RING domain E3 ubiquitin ligases, *Annu Rev Biochem 78*, 399-434.

13. Metzger, M. B., Pruneda, J. N., Klevit, R. E., and Weissman, A. M. (2014) RING-type E3 ligases: master manipulators of E2 ubiquitin-conjugating enzymes and ubiquitination, *Biochim. Biophys. Acta 1843*, 47-60.

14. Zheng, N., Schulman, B. A., Song, L., Miller, J. J., Jeffrey, P. D., Wang, P., Chu, C., Koepp, D. M., Elledge, S. J., Pagano, M., Conaway, R. C., Conaway, J. W., Harper, J. W., and Pavletich, N. P. (2002) Structure of the Cul1–Rbx1–Skp1–F boxSkp2 SCF ubiquitin ligase complex, *Nature 416*, 703-709.

15. Ohta, T., Michel, J. J., Schottelius, A. J., and Xiong, Y. (1999) ROC1, a homolog of APC11, represents a family of cullin partners with an associated ubiquitin ligase activity., *Mol. Cell 3*, 535–541.

16. Seol, J. H., Feldman, R. M., Zachariae, W., Shevchenko, A., Correll, C. C., Lyapina, S., Chi, Y., Galova, M., Claypool, J., Sandmeyer, S., Nasmyth, K., Deshaies, R. J., Shevchenko, A., and Deshaies, R. J. (1999) Cdc53/cullin and the essential Hrt1 RING-H2 subunit of SCF define a ubiquitin ligase module that activates the E2 enzyme Cdc34., *Genes Dev. 13*, 1614–1626.

17. Xu, L., Wei, Y., Reboul, J., Vaglio, P., Shin, T. H., Vidal, M., Elledge, S. J., and Harper, J. W. (2003) BTB proteins are substrate-specific adaptors in an SCF-like modular ubiquitin ligase containing CUL-3., *Nature 425*, 316-321.

18. Bai, C., Sen, P., Hofmann, K., Ma, L., Goebl, M., Harper, J. W., and Elledge, S. J. (1996) SKP1 connects cell cycle regulators to the ubiquitin proteolysis machinery through a novel motif, the F-box., *Cell. 86*, 263-274.

19. Kamura, T., Sato, S., Haque, D., Liu, L., Kaelin, W. G. J., Conaway, R. C., and Conaway, J. W. (1998) The Elongin BC complex interacts with the conserved SOCS-box

motif present in members of the SOCS, ras, WD-40 repeat, and ankyrin repeat families., *Genes Dev. 12*, 3872-3881.

20. Shiyanov, P., Nag, A., and Raychaudhuri. (1999) Cullin 4A associates with the UV-damaged DNA-binding protein DDB., *J. Biol. Chem. 274*, 35309–35312.

21. Kamura, T., Conrad, M. N., Yan, Q., Conaway, R. C., and Conaway, J. W. (1999) The Rbx1 subunit of SCF and VHL E3 ubiquitin ligase activates Rub1 modification of cullins Cdc53 and Cul2. , *Genes Dev. 13*, 2928–2933

22. Liu, Y., Mathias, N., Steussy, C. N., and Goebl, M. G. (1995) Intragenic suppression among CDC34 (UBC3) mutations defines a class of ubiquitin-conjugating catalytic domains. , *Mol. Cell. Biol. 15*, 5635–5644

23. Osaka, F., Saeki, M., Katayama, S., Aida, N., Toh-E.A., Kominami, K., Toda, T., Suzuki, T., Chiba, T., Tanaka, K., and Kato, S. (2000) Covalent modifier NEDD8 is essential for SCF ubiquitin-ligase in fission yeast., *EMBO J 19*, 3475-3484.

24. Hori, T., Osaka, F., Chiba, T., Miyamoto, C., Okabayashi, K., Shimbara, N., Kato, S., and Tanaka, K. (1999) Covalent modification of all members of human cullin family proteins by NEDD8., *Oncogene. 18*, 6829-6834.

25. Schulman, B. A., Carrano, A. C., Jeffrey, P. D., Bowen, Z., Kinnucan, E. R., Finnin, M. S., Elledge, S. J., Harper, J. W., Pagano, M., and Pavletich, N. P. (2000) Insights into SCF ubiquitin ligases from the structure of the Skp1-Skp2 complex., *Nature. 408*, 381-386.

26. Wu, G., Xu, G., Schulman, B. A., Jeffrey, P. D., Harper, J. W., and Pavletich, N. P. (2003) Structure of a beta-TrCP1-Skp1-beta-catenin complex: destruction motif binding and lysine specificity of the SCF(beta-TrCP1) ubiquitin ligase.
, *Mol Cell. 11*, 1445-1456.

27. Orlicky, S., Tang, X., Willems, A., Tyers, M., and Sicheri, F. (2003) Structural basis for phosphodependent substrate selection and orientation by the SCFCdc4 ubiquitin ligase., *Cell. 112*, 243-256.

28. Duda, D. M., Borg, L. A., Scott, D. C., Hunt, H. W., Hammel, M., and Schulman, B. A. (2008) Structural insights into NEDD8 activation of cullin-RING ligases: conformational control of conjugation, *Cell 134*, 995-1006.

29. Liu, J., and Nussinov, R. (2011) Flexible cullins in cullin-RING E3 ligases allosterically regulate ubiquitination. , *J Biol Chem 286*, 40934–40942.

30. Burnatowska-Hledin, M., Zeneberg, A., Roulo, A., Grobe, J., Zhao, P., Lelkes, P. I., Clare, P., and Barney, C. (2001) Expression of VACM-1 protein in cultured rat adrenal endothelial cells is linked to the cell cycle., *Endothelium. 8*, 49-63.

31. Kamura, T., Maenaka, K., Kotoshiba, S., Matsumoto, M., Kohda, D., Conaway, R. C., Conaway, J. W., and Nakayama, K. I. (2004) VHL-box and SOCS-box domains determine binding specificity for Cul2-Rbx1 and Cul5-Rbx2 modules of ubiquitin ligases. , *Genes Dev. 18*, 3055–3065.

32. Mahrour, N., Redwine, W. B., Florens, L., Swanson, S. K., Martin-Brown, S., Bradford, W. D., Staehling-Hampton, K., Washburn, M. P., Conaway, R. C., and Conaway, J. W. (2008) Characterization of Cullin-box sequences that direct recruitment of Cul2-Rbx1 and Cul5-Rbx2 modules to elongin BC-based ubiquitin ligases., *J Biol Chem. 283*, 8005–8013.

33. Okumura, F., Matsuzaki, M., Nakatsukasa, K., and Kamura, T. (2012) The role of elongin BC-containing ubiquitin ligases. , *Front Oncol. 2*, 10.

34. Muniz, J. R., Guo, K., Kershaw, N. J., Ayinampudi, V., von Delft, F., Babon, J. J., and Bullock, A. N. (2013) Molecular architecture of the ankyrin SOCS box family of Cul5-dependent E3 ubiquitin ligases, *J Mol Biol 425*, 3166-3177.

35. Fei, X., Gu, X., Fan, S., Yang, Z., Li, F., Zhang, C., Gong, W., Mao, Y., and Ji, C. (2012) Crystal structure of Human ASB9-2 and substrate-recognition of CKB, *Protein J 31*, 275-284.

36. Thomas, J. C., Matak-Vinkovic, D., Van Molle, I., and Ciulli, A. (2013) Multimeric complexes among ankyrin-repeat and SOCS-box protein 9 (ASB9), ElonginBC, and Cullin 5: insights into the structure and assembly of ECS-type Cullin-RING E3 ubiquitin ligases., *Biochemistry. 52*, 5236-5246.

37. Debrincat, M. A., Zhang, J. G., Willson, T. A., Silke, J., Connolly, L. M., Simpson, R. J., Alexander, W. S., Nicola, N. A., Kile, B. T., and Hilton, D. J. (2007) Ankyrin repeat and suppressors of cytokine signaling box protein Asb-9 targets creatine kinase B for degradation, *J Biol Chem 282*, 4728–4737.

38. Balasubramaniam, D., Schiffer, J., Parnell, J., Mir, S. P., Amaro, R. E., and Komives, E. A. (2015) How the ankyrin and SOCS box protein, ASB9, binds to creatine kinase, *Biochemistry 54*, 1673-1680.

Chapter II

Purification of the CUL5-ASB9 E3 Ligase

A. Background

The Ubiquitin-proteasome pathway is one of the main ways cells recycle proteins. The final step before proteasomal degradation, the attachment of ubiquitin to the target protein, is mediated by the E3 ubiquitin ligase. The Cullin-RING ligase (CRL) family is the most well-characterized of the known E3ligases. The CUL5-RING ligase subfamily typically consist of the protein Cullin 5(CUL5) which serves as a scaffold, the RING-domain containing protein, Rbx2, which binds to the C-terminus of CUL5, and Elongins B & C (EloB/C) which act as adaptors for the substrate receptor. The Ankyrin repeat and SOCS-box (ASB) protein family is known to interact with CUL5-Rbx2, serving as substrate receptors. ASB9 was initially identified bound to the substrate creatine kinase B (CKB) (*1*). Creatine kinase is associated with energy metabolism and overexpression of creatine kinase is often found in tumors, including neuroblastoma, colon adenocarcinoma, and prostate and breast carcinoma (*2*). Further, high levels of ASB9 mRNA have been associated with positive prognosis in colorectal cancer (*3*). On its own, ASB9 is unstable, but binding to EloB/C or its substrate increases its stability. ASB9-Cul5 E3 ligase along with the ubiquitin activating enzyme UBE1 and the ubiquitin conjugating enzyme UBE2D2 ubiquitylate a variety of substrates, notably CKB and uMtCK. Additionally, it is thought that CRL activity requires a modification called neddylation where the ubiquitin-like molecule NEDD8 is attached to a conserved lysine near the CUL5 C-terminal domain (*4*). Like ubiquitylation, neddylation requires its own E1 activating(NAE1) and E2 conjugating (UBE2F) enzymes which neddylate CRL.

To date, there is limited structural or dynamic characterization of ASB-containing E3 ligases. The individual components of ASB9-CUL5 are insoluble and form aggregates when purified separately. Previous studies have shown success expressing and purifying separate

components of the ASB9-CUL5 complex by truncating disordered or insoluble ASB9 and CUL5 regions. (*5*). An attractive method of purification is co-expression/co-purification which allows two or more proteins to interact and thus increases their stability. A study (*6*) showed successful reconstitution and purification of the CUL5-SOCS2 by co-expression of CUL5-Rbx2 and SOCS2-EloB/C. Additionally, these researchers successfully reconstituted both neddylated and unneddylated CUL5-SOCS2 ligase. Other researchers designed a structural model for ASB9-CUL5 based on determined crystal structures of components of CUL5 and ASB9-EloB/C and homology modeling, but incorrectly docked ASB9 with CK. (*7, 8*). Despite these contributions, no extensive biophysical studies or crystal structure for complete ASB9-CUL5 exist. Here I show a novel method for the *in vitro* recombinant expression, purification and reconstitution of both neddylated and unneddylated ASB9-CUL5 using co-expression and His-tag affinity purification. Further, I confirm activity of ASB9-CUL5 through *in vitro* ubiquitylation assays and anti-Ub Western Blots.

B. Materials and Methods

1. DNA Constructs for ASB9-EloB/C and EloB/C-Cul5-Rbx2 Co-expression

All genes used for constructing the co-expression of the entire ASB9-CRL encoded the human protein sequences. Most of the initial cloning was done by Ryan Lumpkin and I did the protein expression. ASB9 was cloned into a pHis8 vector with Kanamycin(KAN) resistance and an N-terminal His-tag as described in (Balasubramanian, 2015). Elongin B (TCEB2A) and Elongin C (TCEB1A) were obtained in a pACYC vector with Chloramphenicol (CAM) resistance from Structural Genomics Consortium. Human CUL5 was originally received in a pRSF-Duet vector with Rbx2, with CUL5 containing an N-terminal His-tag and a GB1 tag. CUL5 was then subcloned into a pET28a(KAN) vector retaining its His-tag and GB1 tag and

adding TEV cleavage site following the His-tag. Rbx2 was subcloned into a pET11a(AMP) vector. The EloB/C co-expression plasmid was transformed into BL21 $RbCl_2$ competent *E. coli* cells, then the cells were transformed with ASB9. ASB9-EloBC (AE) cells were selected by growing on LB-Agar plates containing 50 μg/ml KAN and 200 μg/ml AMP. Similarly, BL21 cells containing the EloB/C co-expression plasmid were transformed with the Rbx2 expression plasmid, made competent, then transformed again the with CUL5 expression plasmid. The cells co-expressing EloB/C-CUL5-Rbx2(ECR) were selected by growing on LB-Agar plates containing 200 μg/ml AMP, 34 μg/ml CAM, and 50 μg/ml KAN.

2. DNA Constructs for UbE1, UbE2D2, Ub, NAE1, UbE2F, and Nedd8.

The gene for human UBE1 with an N-terminal His-tag was obtained from Addgene (#34965) and ligated into the pET21d(AMP) vector. The human ubiquitin gene (Ub) was obtained in a pAED4-Ub vector and subcloned into a pET28a(KAN) vector. The gene for human UBE2D2 was obtained from Addgene (#60443) and I ligated into a pETSUMO(KAN) vector adding an N-terminal His-tag and N-terminal SUMO tag. Human NAE1(UBA3) was obtained as gift from Brenda Schulman in a pGEX4T1(AMP) vector with a GST-tag. Human Nedd8(N8) was obtained from Addgene (#18711) and subcloned into pET28a vector with an N-terminal His-tag. Human UBE2F was obtained from Addgene (#15800) in a pDEST17 vector and subcloned into a pET28a vector with an N-terminal His-tag. The Ub and N8 expression vectors were subcloned into pET28a plasmids containing UBE1 and NAE1, respectively. All subcloned vectors were confirmed with DNA sequencing. The UBE1-Ub co-expression vector was co-transformed into BL21 cells and plated on LB-Agar plates with 200 μg/ml AMP+ 34 μg/ml CAM. The NAE1-N8 co-expression vector was transformed into BL21 cells and plated on LB-Agar plates with 200 μg/ml AMP + 50 μg/ml KAN. The Ub, Nedd8, UBE2D2 and UBE2F

expression vectors were respectively transformed into BL21 cells and plated on LB-Agar plates with 50 μg/ml KAN.

3. DNA Constructs for Histones H2A, H2B, H3 and H4

Genes for *Xenopus laevis* histones H2A, H2B, H3 and H4 were obtained as a gift from Dominic Narang in separate pET28a(KAN) vectors. Each plasmid was transformed into BL21 *E. coli* cells and plated onto LB-Agar plates (50 μg/ml KAN).

4. E3 Ligase and Ubiquitin Machinery Protein Expression and Purification

All proteins were expressed as follows: Protein growth began with 5mL overnight cultures of AE and ECR inoculated with a single colony from their selected plates and grown at 37°C in M9-Zn(1.5x M9, 0.8% dextrose, 1mM $MgSO_4$, 0.2mM $CaCl_2$) media. A 20 mL M9-Zn starter culture was inoculated using 2 mL of overnight culture and grown for 2 hours at 37°C. Then, 1L M9 growth cultures (1.5x M9, 1% m/v tryptone, 0.8% dextrose, 1mM $MgCl_2$, 0.2mM $CaCl_2$) were inoculated with the 20 mL starter cultures and grown until OD_{600}= 1.0. After placing the cultures on ice for 30 minutes, protein expression was induced by adding 0.5mM IPTG. Cultures containing Rbx2 were brought to 250μM $ZnCl_2$ because Rbx2 contains a Zinc-binding domain. Cultures were transferred to an 18°C incubator for 16-20 hours.

Cells were pelleted by centrifugation at 5000rpm for 10 minutes and resuspended in 50 mL resuspension buffer (50mM Tris-HCl pH 8.0, 100mM NaCl, 10mM Imidazole pH 8.0, 2mM β-mercaptoethanol (BMe), 5% Glycerol) with protease inhibitor cocktail and 5mM phenylmethylsulfonylfluoride (PMSF). Cells were lysed on ice by sonication with 10 rounds of 30 second pulses and 45 seconds between each pulse. Lysate was clarified by centrifugation at 13000 rpm for 45 minutes. The clarified lysate was incubated with 2 mL Ni-NTA slurry (Thermo-Fisher) for 2 hours at 4°C. The lysate-slurry mix was then collected in a gravity

filtration column (Bio-rad, 20x2 cm) at 4°C. The column containing Ni-NTA beads was washed with 20 mL resuspension buffer and 20 mL wash buffer (50mM Tris-HCl pH 8.0, 100mM NaCl, 25mM Imidazole pH 8.0, 2mM BMe, 5% Glycerol, 250μM $ZnCl_2$). Protein was eluted from the Ni-NTA beads with 20 mL elution buffer (50mM Tris-HCl pH 8.0, 100mM NaCl, 250mM Imidazole pH 8.0, 2mM BMe, 5% Glycerol, 250uM ZnCl). Proteins were dialyzed overnight in a 12-14 kDa cutoff dialysis tubing in dialysis buffer (20mM Tris-HCl pH 8.0, 100mM NaCl, 1mM DTT, 5% Glycerol, 250 μM ZnCl) with stirring at 4°C. Proteins were concentrated to 2mL and purified using size-exclusion chromatography over a Superdex S200 16x200 column in dialysis buffer. Peak fractions were collected and combined.

For preparation of the ASB9-EloBC-CUL5-Rbx2(AECR) complex, cell pellets of AE and ECR were combined in a 1:2 ratio and purification was performed as described in the previous paragraph. Preparation of ASB9-EloBC-Cul5-Rbx2-Nedd8(AECR-N8) was as follows: Cell pellets of AE, NAE1-N8 and ECR were combined in a 1:1:2 ratio and resuspended in 100 mL resuspension buffer. Purification continued as before until the Ni-NTA incubation, where the Ni-NTA/lysate mix was spiked with 5mM $MgCl_2$ and 2mM ATP. Purification was carried out as described previously until post-dialysis, where the 20 mL sample was brought to 5 mM $MgCl_2$ and 2mM ATP and spiked with 1mg of UBE2F, and then incubated for 2 hours at 4°C. The sample was then concentrated and purified as described previously. All proteins were visualized and verified by 10-15% SDS-PAGE gels and mass spectrometry.

5. Protein Expression and Purification for Histones

Histones H2A, H2B, H3 and H4 were purified individually as follows: Histone plasmids were transformed into BL21 (DE3) pLysS competent cells and overnight cultures were started in 10mL LB broth at 37°C with shaking. Overnight cultures were used to inoculate 1L 2YT

cultures and were grown at 37°C with shaking until they reached OD_{600} between 0.4-0.6. Cultures were induced in 0.2mM IPTG and grown for another 3 hours. Cells were centrifuged at 5000rpm for 10 minutes at 4°C and cell pellets were resuspended with 35mL wash buffer (50mM Tris pH 7.5, 100mM NaCl, 1mM EDTA, 1mM BME, 1mM Benzamidine), then sonicated for eight 1-minute pulses (2 minutes between each pulse) on ice. Lysate was clarified by centrifugation at 13000 rpm for 20 minutes. Inclusion bodies were collected and washed with 25mL wash buffer with 1% Triton X-100 and centrifuged for 20 minutes. Washing was repeated three more times, but without Triton X-100. The inclusion body pellets were minced and dissolved in 0.25mL DMSO with a spatula and incubated at 25°C for 30 minutes. 6 mL of unfolding buffer (6M Guanidine, 20mM Tris pH 7.5, 5mM DTT) was added to the sample and stirred for 2 hours at 25°C then centrifuged for 30 minutes at 13000rpm. The unfolded samples were purified by size exclusion chromatography over a Sephacryl S200 16/60 column in size exclusion buffer (7M Urea, 20mM NaAc pH 5.2, 0.2M NaCl, 2mM Bme). The peak fractions were pooled and placed in 6-8 kDa MWCO dialysis tubing and dialyzed for 3-hour rounds in dialysis buffer (MQ water, 2mM Bme) followed by lyophilization in 2mg aliquots and stored at -80°C. Samples were further purified by ion-exchange chromatography using an SP Sepharose column, resuspended in buffer A(7M Urea, 20mM NaAc pH 5.2, 0.2 NaCl, 2mM Bme) and eluted by an increasing linear gradient from 0 to 100% of buffer B (7M Urea, 20mM NaAc, pH 5.2, 0.6M NaCl, 2mM Bme). Samples were dialyzed and lyophilized as previously described.

Histone octamers and tetramers were formed as follows: one 2mg aliquot for each histone monomer was thawed and dissolved in 1mL unfolding buffer (6M Guanidine, 20mM Tris pH 7.5, 5mM DTT) and incubated at 25°C for 45 minutes. Concentrations for each sample were measured by UV-Vis absorbance at 280nm and the different histones were combined in a 1:1

molar ratio (H3:H4) for tetramer formation or a 1:1:1:1 molar ratio (H2A:H2B:H3:H4) for octamer formation. Samples were diluted to 1mg/mL and dialyzed in refolding buffer (2M NaCl, 10mM Tris pH 7.5, 1mM EDTA, 1mM DTT) for three 3-hour rounds. Samples were purified by size exclusion chromatography over a Sephadex 200 column in refolding buffer. Samples were concentrated to ~20μM and immediately used or stored at -80°C.

6. Activity Assays

Transfer of Ub by thioesterification from UBE1 to UBE2D2 was carried out in a reaction buffer (20mM Tris pH 7.5, 5mM $MgCl_2$, 0.5mM DTT, and 2mM ATP) with the following protein concentrations: 1μM UBE1, 1μM UBE2D2, and 5μM Ub in total volume of 40μL. Thioester reactions were incubated at 25°C for 5 minutes. Reactions were quenched with non-reducing SDS-PAGE buffer and boiled at 90°C for 10 minutes. Reaction samples were separated on 10% Polyacrylamide gels and visualized with Coomassie Blue staining.

Ubiquitylation assays were carried out in reaction buffer(20mM Tris pH 7.5, 5mM $MgCl_2$, 0.5mM DTT, and 2mM ATP) with the following protein concentrations: 0.1μM UBE1, 1μM UBE2D2, 30μM Ub, 1μM ASB9-CUL5, 1μM ASB9-CUL5-N8 and 2μM *Xenopus laevis* Histone Octamers in 40uL and incubated for 2 hours at 25°C. Reactions were quenched with SDS-PAGE reducing buffer and boiled at 90°C for 10 minutes. Reactions were separated on 15% Polyacrylamide gels and visualized with Coomassie blue staining.

7. Western Blots

Ubiquitylation reaction samples were transferred from acrylamide gel to nitrocellulose using electrophoretic transfer in cold transfer buffer(25mM Tris Base, 200mM Glycine, 20% Methanol) at 100 V for 30 minutes in a Biorad Miniprotean western blot apparatus. Nitrocellulose was blocked with a blotto mixture of TBS(150mM NaCl, 50 mM Tris pH 7.5) and

1mg/mL casein for 1 hour and incubated with primary anti-Ub antibody in blocking solution(1μg/mL primary antibody, 150mM NaCl, 50 mM Tris pH 7.5). Nitrocellulose was then washed in TTBS(TBS with 0.05% Tween-20) and incubated with a solution containing secondary anti-rabbit antibody (1μg/mL secondary antibody, 150mM NaCl, 50 mM Tris pH 7.5) for 1 hour. Nitrocellulose was washed with TTBS and followed by TBS to remove any remaining surfactant. The blot was developed with Bio-Rad Clarity Western ECL Substrate and imaged with a Bio-Rad Chemi-Doc provided by the Bennet lab located on the 6th floor of the Natural Sciences Building, UCSD.

C. Results

1. Purification of AECR by Affinity Chromatography Yields a Fully Reconstituted Ligase

Our purification strategy was based on co-expression of individual AECR components to increase their stability. Components like ASB9 are not very stable on their own, but co-expression with EloB/C in E. coli increased their stability during recombinant expression and purification. Similarly, CUL5 is unstable on its own, but became much more soluble when co-expressed with EloB/C and Rbx2. In Figure 2.1a, Lanes 7-10 show the Ni-NTA affinity purification for AECR. We observed that despite only CUL5 and ASB9 containing His-tags, EloB/C are not removed during the wash steps. These results show that EloB/C interact with high affinity to ASB9 and CUL5 such that they remain bound through the wash steps. Rbx2 is about 12 kDa, so it was not seen on the gel. AECR-N8 was similarly purified by combining AE and ECR with NAE1 and NEdd8 immediately after lysis. Samples were spiked with 5 mM $MgCl_2$ and 2mM ATP to ensure the thioester bond formation between NAE1 and Nedd8. In Figure 2.1a, lanes 3-6 show the Ni-NTA purification process for AECR-N8. Note that the NAE1 may not have a high enough concentration to be visualized during Ni-NTA purification.

Following Ni-NTA affinity purification, AECR was dialyzed and further purified by size-exclusion chromatography (see Methods for details). Using this technique, we were able to isolate AECR with high resolution and confirm its molecular weight according to when it eluted. This process is illustrated in Figure 2 which shows the chromatograms for the purification of AECR and AECR-N8. The addition of the 9kDa protein Nedd8, results in AECR-N8 eluting at an earlier volume than AECR. Figure 1b confirms the isolation of AECR-N8 and AECR by SDS-PAGE analysis. Size exclusion samples show about a 9 kDa shift between neddylated and unneddylated CUL5, confirming its Neddylation. All other proteins needed for ubiquitylation and neddylation reactions were purified using the same scheme. UBE2D2 and UBE2F were found to be highly stable during purification, often yielding >2mg/mL concentrations from a 1L cell culture. The yield of UBE1 was lower comparatively, but we obtained sufficient amounts for later experiments. NAE1 and Nedd8 were purified in-tandem with AECR when needed.

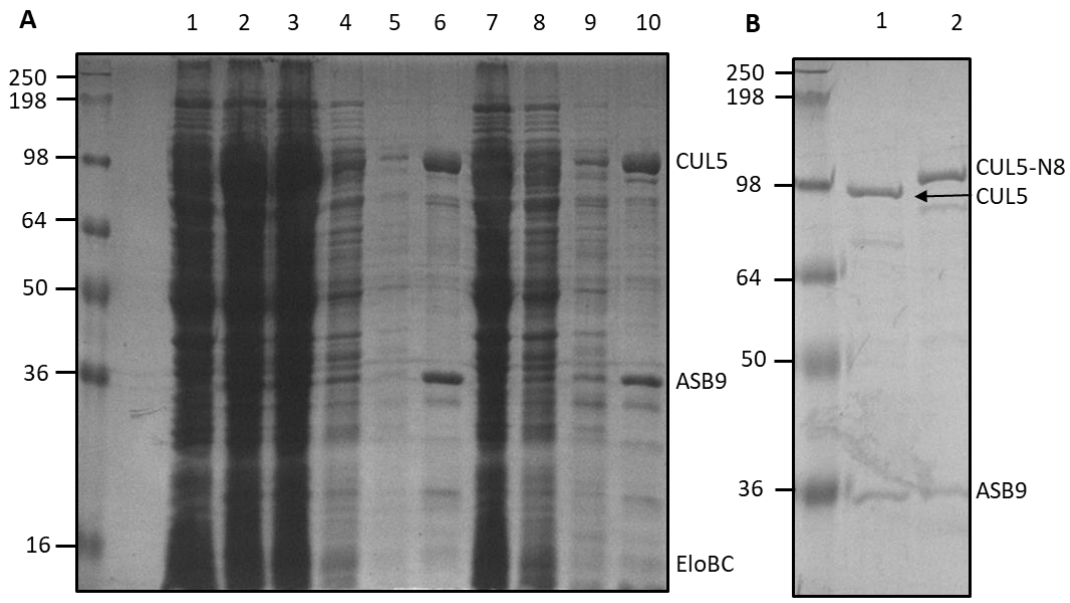

Figure 2.1: SDS-PAGE Analysis of AECR and AECR-N8. A) Samples were taken at each step during the purification process. Lanes 1-2 are cell lysate pellet and soup. Lanes 3-6 are AECR with NAE1 and Nedd8. Lanes 7-10 are AECR without NAE1 and Nedd8. Lanes 3 and 7 are flow-through during Ni-NTA purification. Lanes 4 and 8 are resuspension buffer flow-through. Lanes 5 and 9 are wash buffer flow-through. Lanes 6 and 10 are eluent. B) Size-exclusion samples of AECR and AECR-N8. Lane 1 is AECR. Lane 2 is AECR-N8. Lane 2 shows a ~9 kDa band shift which corresponds to neddylated Cullin 5.

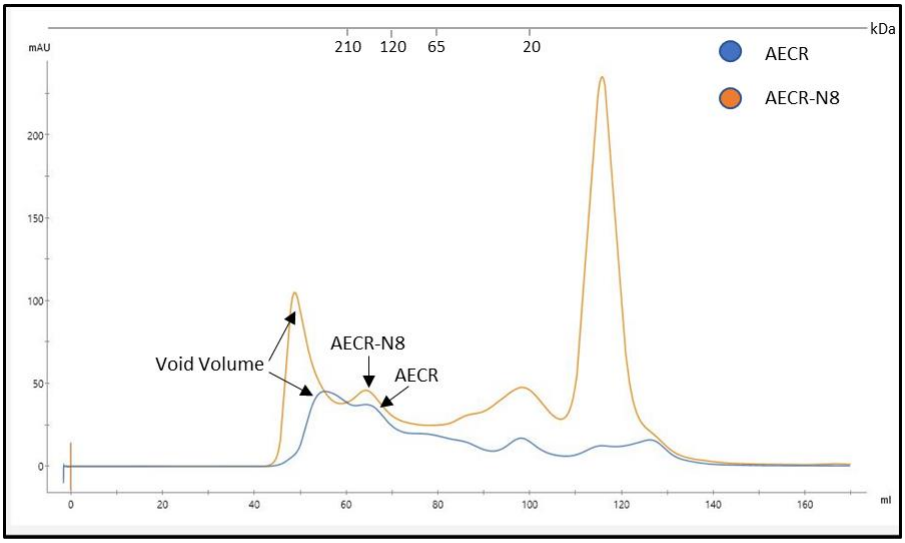

Figure 2.2: Size Exclusion Chromatogram of AECR and AECR-N8. Blue, AECR; Orange, AECR-N8. Peaks between 45mL and 60mL are void volumes. Peaks at 65mL correspond to a molecular weight of 160kDa which matches AECR or AECR-N8 molecular weights. The sharp orange peak at ~116mL is excess Nedd8.

2. Ubiquitylation Assay with Histone Octamers Confirms Activity of Recombinant Ubiquitin Machinery

After purification, we tested the activity of our ubiquitylation cascade enzymes through activity assays and SDS-PAGE analysis. A thioester assay in non-reducing SDS dye showed formation of a thioester bond between UBE2D2 and Ub, confirming UBE1 activity. Next, we tested ubiquitylation activity of AECR and AECR-N8 with *Xenopus* histone octamers as a substrate. Figure 3 shows an SDS-PAGE analysis of our activity assay. Lanes 1-4 show the position of each protein in the reaction solution. Lanes 5 and 6 which contain all components but the octamer substrate, showed higher-order bands at the 98 kDa marker and beyond, indicative of mono or poly-ubiquitylation of the ligase proteins. This result suggests components of both AECR and AECR-N8 are auto-ubiquitylated when no substrate is present. Lane 7 served as a negative control for E3 independent ubiquitylation. It has been shown that E2 enzymes are capable of ubiquitylation on their own, so it was necessary to confirm UBE2D2 is not the ubiquitylating enzyme in this cascade. Lanes 8 and 9 revealed higher order bands in the 36-98 kDa range, distinct from those seen in lanes 5-6. Based on their molecular weights, these bands appear to be mono- or polyubiquitylated histone monomers or ASB9. Presence of these unique bands suggest our AECR and AECR-N8 complexes are active and capable of ubiquitylating histone octamer substrates. Higher order bands above the 98 kDa marker are still present but show lighter intensity which indicates AECR still auto-ubiquitylates when substrate is present.

To further confirm ubiquitylation activity, we performed an anti-Ub Western Blot on our SDS-PAGE gel to confirm the presence of ubiquitin in these higher order bands. Indeed, Figure 2b reveals the presence of ubiquitin in the higher-order bands, confirming that our recombinant AECR and AECR-N8 E3 ligases ubiquitylate itself or its octamer substrate. Some non-specific

antibody binding was observed, notably toward CUL5. This can be attributed to the presence of a GB 1 domain which is part of the fusion construct used to produce CUL5.

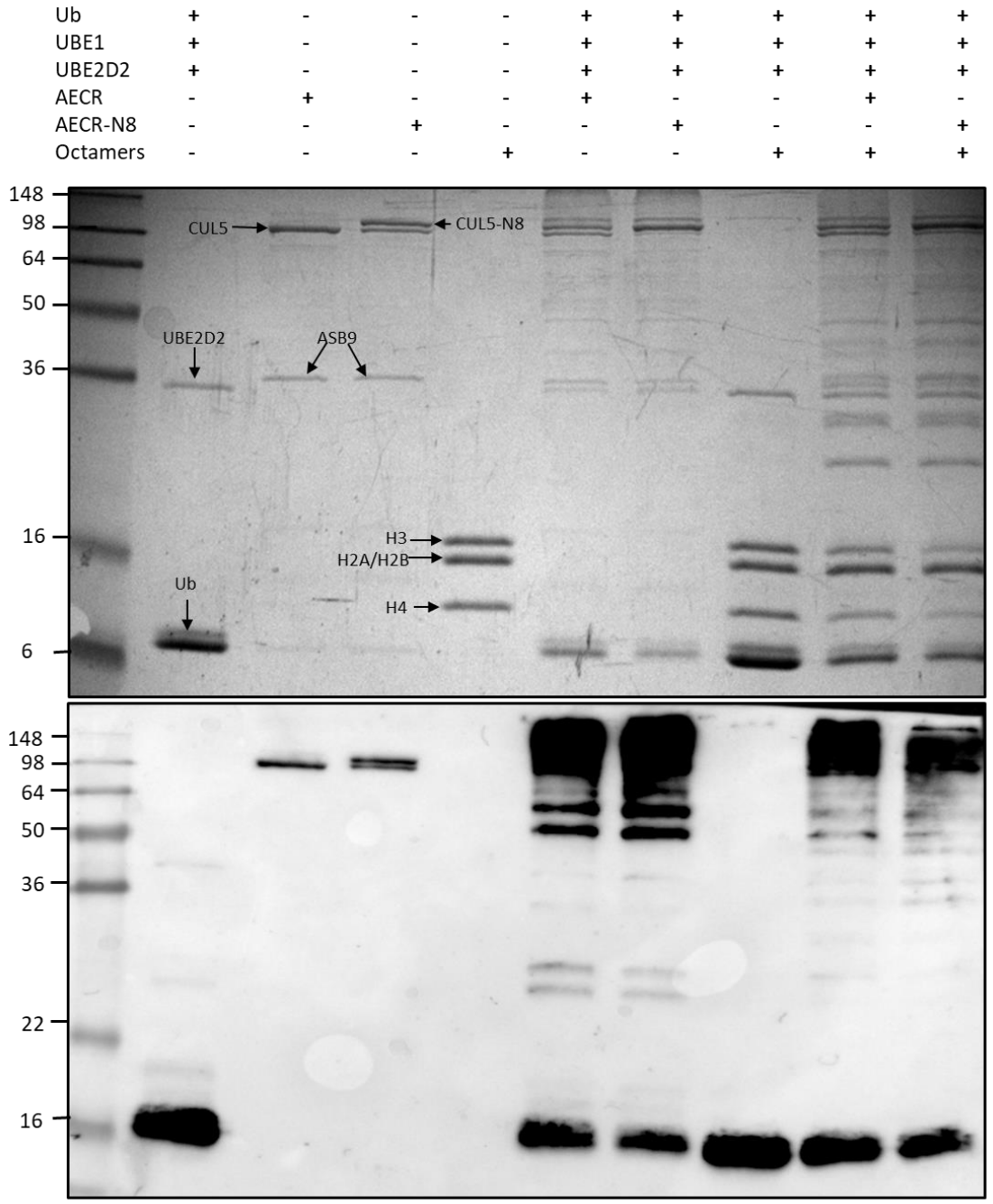

Figure 2.3: A) Ubiquitylation Assay of Histone Octamers with AECR and AECR-N8. Lanes 2-5 are references for protein position on the gel. Bands are labeled by markers. Lanes 6 and 7 are a control for auto-ubiquitylation of AECR/AECR-N8. Lane 8 is a control for E3-independent Ubiquitylation. Lanes 9 and 10 are ubiquitylation of histone octamers with AECR and AECR-N8, respectively. **B) Anti-Ub Western Blot of Histone Octamers with AECR and AECR-N8.** Contents of each lane are identical to the SDS-PAGE gel. Non-specific binding to CUL5 can be seen in lanes 3 and 4.

D. Discussion

1. CUL5 Neddylation Has No Observable Effect on Histone Ubiquitylation Patterns

We tested the activity of AECR and AECR-N8 through a ubiquitylation assay with histone octamers. A previous study (*9*) showed via crystal structures and MD simulations, that neddylation may have an allosteric effect on CUL5- Rbx1 by bringing the E2-Ub complex in closer proximity to the substrate receptor for polyubiquitylation. They further claim that neddylation-driven RING domain rotations in Rbx1 are necessary for initiating poly-ubiquitylation, suggesting this as a reason for the observed inactivity in unneddylated CRLs. However, this hypothesis conflicts with our results. Not only did I observe ubiquitylation activity in unneddylated CUL5, but the pattern of ubiquitylation appears identical from SDS-PAGE analysis (Fig. 2.3a). Three discrete bands in both neddylated and unneddylated reactions can be seen above the 16 kDa marker, which correspond to 8.5 kDa shifts from the H2A/B, H3 and H4 locations on the gel. These bands which are not present in any other lane, are indicative of monoubiquitylated histone substrates. Lanes 9 and 10 also contain new bands from 36 kDa onward, suggesting the presence of polyubiquitylated substrates. There are similarities between the 36-50 kDa range of bands in lanes 9-10 compared to 5-6, though the bands in lanes 9-10 appear darker and more defined. An anti-Ub Western blot of the SDS-PAGE gel further confirms the presence of ubiquitylated histones in these higher order bands. This ubiquitylation assay shows there is much to be understood regarding the purpose of neddylation and opens the possibility that neddylation may not be required for CUL5 ubiquitylation.

2. Histone Octamers are A Novel Substrate for ASB9-Cul5 E3 Ligase

Previous proteomics studies of SOCS-box containing proteins have shown CKB to be the predominant binding partner for ASB9 and have shown CKB is polyubiquitylated in an ASB9-dependent manner (*1*). However, a recent proteomics study (*10*) of ASB family members

revealed ASB9 as a binding partner for all four histone monomers. Thus, I decided histone octamers may be a worthwhile substrate to test the activity of AECR. Indeed, our SDS-PAGE gel shows evidence of mono- and polyubiquitylation of the histone monomers. To date, most studies of ASB9 have focused on interactions with CKB. Our studies are the first demonstration of *in vitro* ubiquitylation by the ASB9-CUL5 E3 ligase. These results suggest ASB9 may be a flexible substrate receptor, capable of interacting with multiple substrates and targeting them for ubiquitylation. Further, this may indicate ASB9 regulates multiple different pathways *in vivo*, considering it can facilitate ubiquitylation of two vastly different substrates.

E. Conclusions

Together with Ryan Lumpkin, I developed a recombinant expression and purification of the ASB9-Cul5 E3 Ubiquitin ligase and demonstrated its activity via in vitro ubiquitylation assay of histone octamers. This was the first time anyone had assembled an active CUL5 E3 ligase completely *in vitro*. I showed that ASB9 can recognize and ubiquitylate histone octamers independent of CUL5 neddylation. Determining the effects of neddylation in relation to ubiquitylation *in vitro* provide insight to the significance of neddylation and elucidate the dynamic mechanism of ubiquitylation by CRLs.

Chapter II, in full, is currently being prepared for submission for publication of the material. Lumpkin, Ryan J.; Condon, Christopher J. The thesis author significantly contributed to this work as a researcher and author.

F. References

1. Debrincat, M. A., Zhang, J. G., Willson, T. A., Silke, J., Connolly, L. M., Simpson, R. J., Alexander, W. S., Nicola, N. A., Kile, B. T., and Hilton, D. J. (2007) Ankyrin repeat and suppressors of cytokine signaling box protein Asb-9 targets creatine kinase B for degradation, *J Biol Chem 282*, 4728–4737.

2. Wyss, M., and Kaddurah-Daouk, R. (2000) Creatine and creatinine metabolism, *Physiol Rev 80*, 1107–1213.

3. Tokuoka, M., Miyoshi, N., Hitora, T., Mimori, K., Tanaka, F., Shibata, K., Ishii, H., Sekimoto, M., Doki, Y., and Mori, M. (2010) Clinical significance of ASB9 in human colorectal cancer, *Int J Oncol 37*, 1105–1111.

4. Saha, A., and Deshaies, R. J. (2008) Multimodal activation of the ubiquitin ligase SCF by Nedd8 conjugation, *Mol Cell 32*, 21–31.

5. Thomas, J. C., Matak-Vinkovic, D., Van Molle, I., and Ciulli, A. (2013) Multimeric complexes among ankyrin-repeat and SOCS-box protein 9 (ASB9), ElonginBC, and Cullin 5: insights into the structure and assembly of ECS-type Cullin-RING E3 ubiquitin ligases., *Biochemistry. 52*, 5236-5246.

6. Bulatov, E., Martin, E. M., Chatterjee, S., Knebel, A., Shimamura, S., Konijnenberg, A., Johnson, C., Zinn, N., Grandi, P., Sobott, F., and Ciulli, A. (2015) Biophysical studies on interactions and assembly of full-size E3 ubiquitin ligase: suppressor of cytokine signaling 2 (SOCS2)-elongin BC-cullin 5-ring box protein 2 (RBX2), *J Biol Chem 290*, 4178-4191.

7. Duda, D. M., Borg, L. A., Scott, D. C., Hunt, H. W., Hammel, M., and Schulman, B. A. (2008) Structural insights into NEDD8 activation of cullin-RING ligases: conformational control of conjugation, *Cell 134*, 995-1006.

8. Muniz, J. R., Guo, K., Kershaw, N. J., Ayinampudi, V., von Delft, F., Babon, J. J., and Bullock, A. N. (2013) Molecular architecture of the ankyrin SOCS box family of Cul5-dependent E3 ubiquitin ligases, *J Mol Biol 425*, 3166-3177.

9. Onel, M., Sumbul, F., Liu, J., Nussinov, R., and Haliloglu, T. (2017) Cullin neddylation may allosterically tune polyubiquitin chain length and topology, *Biochem J 474*, 781-795.

10. Andresen, C. A., Smedegaard, S., Sylvestersen, K. B., Svensson, C., Iglesias-Gato, D., Cazzamali, G., Nielsen, T. K., Nielsen, M. L., and Flores-Morales, A. (2014) Protein interaction screening for the ankyrin repeats and suppressor of cytokine signaling (SOCS) box (ASB) family identify Asb11 as a novel endoplasmic reticulum resident ubiquitin ligase, *J Biol Chem 289*, 2043-2054.

Chapter III

Characterization of ASB9-CUL5-Mediated Histone Ubiquitylation by LC-MS/MS Mass Spectrometry

A. Background

The Ankyrin and SOCS-box containing (ASB) family of proteins are known to be substrate receptors for the Cullin-RING ligase(CRL) family of ubiquitin E3 ligases containing Cullin 2 or Cullin 5(CUL5) and Elongins B and C(EloBC). A defining feature of CUL5-RING ligases is the presence of a SOCS-box motif on the substrate receptor that binds EloBC, which in turn bind to the C-terminus of CUL5. ASB proteins contain an N-terminal Ankyrin repeat domain which mediate binding to substrates and bring them in proximity to the ligase for ubiquitylation. Though ASB proteins are known to act as ubiquitin ligases, their substrates are not well-characterized.

ASB9 is one of the more extensively studied proteins of the ASB family. ASB9 was initially identified as binding partner for Brain-type Creatine Kinase (CKB) and they were found to share similar levels of expression predominantly in the testes and kidneys. Additionally, they found that polyubiquitylation and proteasomal degradation of CKB occurs in an ASB9-dependent manner (*1*) Biophysical studies have gone on to show that CKB binds as a dimer to ASB9 at the Ankyrin-repeat domain where the first Ankyrin repeat inserts itself between the cleft of the CKB monomers, inhibiting CKB activity (*2*, *3*). Since then, no other binding partners for ASB9 were identified until a proteomics study of the ASB family found that ASB9 binds to a diverse set of proteins (*4*). Among the identified proteins were known interacting partners like various types of CK, but most notably the histone monomers H2A, H2B, H3 and H4 were all identified as interacting partners. The Cullin4A-type E3 ligase has been known to ubiquitylate histones (*5*), but no ASB- type CRLs have been shown to interact.

Histones typically form an octamer consisting of two H2A/H2B dimers and an H3/H4 tetramer. These octamers contain a high amount of lysines and arginines on their surface, making

them highly positively charged. In vivo, dsDNA wraps around histone octamers at roughly 146bp per octamer, forming nucleosomes (*6*). Nucleosomes can further condense into higher-order structures like chromatin, and eventually chromosomes. Nucleosomes are subject to a variety of post-translational modifications (PTMs) that can alter the structure of chromatin by either tightening the interactions between DNA or loosening them. Nucleosomes undergo all types of PTMs, including ubiquitylation, which can induce signals in the cell such as chromatin condensation or DNA-damage response (*7*). My previous experiments recombinantly expressing and purifying the ASB9-EloBC-CUL5-Rbx2 E3 ligase (AECR) have shown AECR is capable of ubiquitylating histone octamers in an *in vitro* ubiquitylation assay. I aim to further characterize the ubiquitylation of the histone octamers by Tandem Mass Spectrometry. I also describe experiments I performed to explore where and how auto-ubiquitylation is occurring on CUL5 by site-directed mutagenesis.

B. Materials and Methods

1. Site-Directed Mutagenesis of CUL5 K724R Plasmid and Protein Purification

Human CUL5 was originally received in a pRSF-Duet vector with Rbx2, with CUL5 containing an N-terminal His-tag and a GB1 tag. CUL5 was then subcloned into a pET28a(KAN) vector retaining its His-tag and GB1 tag and adding TEV cleavage site following the His-tag. The CUL5 plasmid was then mutated at K724 to R using the Quikchange(Agilent) site-directed mutagenesis method with strategically designed primers and PCR. The PCR products were then transformed into DH5α competent *E. coli* cells and plated onto LB-Agar plates (1:1000 KAN). The CUL5 K724R DNA was then sequenced for confirmation of mutagenesis. Expression, purification and reconstitution of all other proteins are identical to as described in Chapter 2 Methods.

2. Activity Assays

Ubiquitylation assays were performed identically as described in Chapter 2 Methods.

3. In-gel Acetylation and Digest of Reaction Samples

The gel slices were cut to 1mm by 1 mm cubes and destained 3 times by first washing with 100 ul of 100 mM ammonium bicarbonate for 15 minutes, followed by addition of the same volume of acetonitrile (ACN) for 15 minutes. The supernatant was discarded and samples were dried in a speedvac. The samples were then acylated with 5µL of acetic anhydride-d6 and 10µL of 0.1M ammonium bicarbonate to improve Trypsin digestion. The pH of the sample mixture was kept between 7-8 with addition of a few microliters of ammonium bicarbonate. The samples were then incubated for 60 minutes at 37°C. Samples were then reduced by mixing with 200 µl of 100 mM ammonium bicarbonate-10 mM DTT and incubated at 56°C for 30 minutes. The liquid was removed and 200 ul of 100 mM ammonium bicarbonate-55mM iodoacetamide was added to gel pieces and incubated at room temperature in the dark for 20 minutes. After the removal of the supernatant and one wash with 100 mM ammonium bicarbonate for 15 minutes, same volume of ACN was added to dehydrate the gel pieces. The solution was then removed and samples were dried in a speedvac. For digestion, enough solution of ice-cold trypsin (0.01 ug/ul) in 50 mM ammonium bicarbonate was added to cover the gel pieces and set on ice for 30 min. After complete rehydration, the excess trypsin solution was removed, replaced with fresh 50 mM ammonium bicarbonate, and left overnight at 37°C. The peptides were extracted twice by the addition of 50 µl of 0.2% formic acid and 5 % ACN and vortex mixing at room temperature for 30 min. The supernatant was removed and saved. A total of 50 µl of 50% ACN-0.2% formic acid was added to the sample, which was vortexed again at room temperature for 30 min. The supernatant was removed and combined with the supernatant from the first extraction. The

combined extractions are analyzed directly by liquid chromatography (LC) in combination with tandem mass spectroscopy (MS/MS) using electrospray ionization.

4. LC-MS/MS Analysis

Trypsin-digested peptides were analyzed by ultra high pressure liquid chromatography (UPLC) coupled with tandem mass spectroscopy (LC-MS/MS) using nano-spray ionization. The nanospray ionization experiments were performed using a Orbitrap fusion Lumos hybrid mass spectrometer (Thermo) interfaced with nano-scale reversed-phase UPLC (Thermo Dionex UltiMate™ 3000 RSLC nano System) using a 25 cm, 75-micron ID glass capillary packed with 1.7-µm C18 (130) BEH^{TM} beads (Waters corporation). Peptides were eluted from the C18 column into the mass spectrometer using a linear gradient (5–80%) of ACN (Acetonitrile) at a flow rate of 375µl/min for 1h. The buffers used to create the ACN gradient were: Buffer A (98% H_2O, 2% ACN, 0.1% formic acid) and Buffer B (100% ACN, 0.1% formic acid). Mass spectrometer parameters are as follows; an MS1 survey scan using the orbitrap detector (mass range (m/z): 400-1500 (using quadrupole isolation), 120000 resolution setting, spray voltage of 2200 V, Ion transfer tube temperature of 275°C, AGC target of 400000, and maximum injection time of 50 ms) was followed by data dependent scans (top speed for most intense ions, with charge state set to only include +2-5 ions, and 5 second exclusion time, while selecting ions with minimal intensities of 50000 in which the collision event was carried out in the high energy collision cell (HCD Collision Energy of 30%), and the fragment masses were analyzed in the ion trap mass analyzer (With ion trap scan rate of turbo, first mass m/z was 100, AGC Target 5000 and maximum injection time of 35ms). Protein identification and label free quantification was carried out using Peaks Studio X (Bioinformatics solutions Inc.) DiGLY-modified peptides were

selected based on a P value < 0.01 for peptide confidence and an Ascore of > 15 based on PTM confidence as described (*8*).

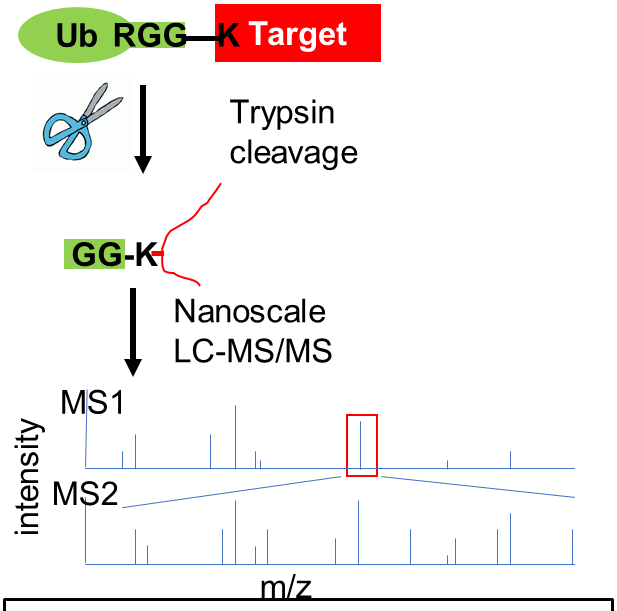

Figure 3.1: Diagram of Diglycyl Lysine detection by LC-MS/MS. Peptides were digested Trypsin and identified by LC-MS/MS

C. Results

1. AECR Preferentially Ubiquitylates Histones H3 and H4

To identify ubiquitylated substrates, we performed a ubiquitylation assay with AECR, AECR-N8, and a histone octamer substrate. Ubiquitylation reactions were visualized by SDS-PAGE which can be seen in Figure 4.1. Lanes 1-5 indicated the relative positions of the ubiquitin machinery and histone octamers. Lanes 6-7 served as controls to see if AECR and AECR-N8 auto-ubiquitylate themselves in the absence of substrates. Indeed, ubiquitylations bands appeared from the 36 kDa marker onward, indicating that AECR and AECR-N8 appear to ubiquitylate ASB9 and CUL5. This was confirmed by comparing band intensities of ASB9 and CUL5 between lanes 3-4 and 6-7 and observing that lanes 6-7 bands are lighter than those in 3-4. Lane 8 served as a control for E3-independent ubiquitylation because E2 enzymes have been known to

catalyze ubiquitin transfer by themselves. The absence of Ub bands confirmed that the ubiquitylation reaction is E3-dependent. Surprisingly, Lanes 9-10 containing histone ubiquitylation reactions with AECR and AECR-N8 showed identical banding, indicating that histone octamer ubiquitylation is not dependent on neddylation. Both lanes 9-10 showed intense banding starting at about 20 kDa onward, with unique bands not observed in any other lanes. Specifically, the bands indicated by the S1 and S2 labeled arrows in Fig. 4.2 correspond to molecular weights of mono-ubiquitylated histones. Additionally, the band intensities of the histone monomers in lanes 9-10 are much lower compared to the intensities of other lanes. Other unique bands are further indicated by the S3-7 labeled arrows in Fig 4.2. Interestingly, the amount of auto-ubiquitylation seemed to decrease in lanes 9-10 when histones were present, as the band intensities for CUL5 and ASB9 are higher than in lanes 6-7.

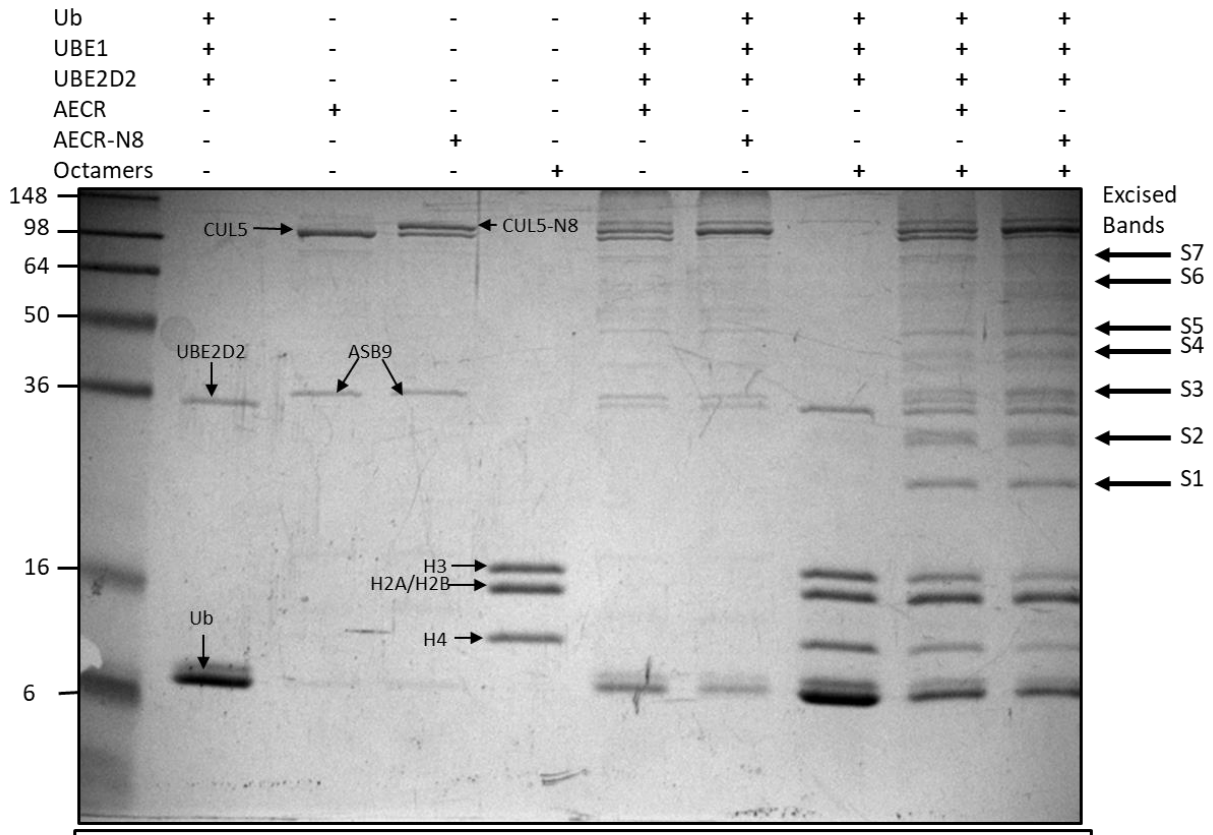

Figure 3.2: Ubiquitylation Assay of Histone Octamers with AECR and AECR-N8. Lanes 2-5 are references for protein position on the gel. Bands are labeled by markers. Lanes 6 and 7 are a control for auto-ubiquitylation of AECR/AECR-N8. Lane 8 is a control for E3-independent Ubiquitylation. Lanes 9 and 10 are ubiquitylation of histone octamers with AECR and AECR-N8, respectively. Excised gel bands for MS/MS are indicated on the right.

Next, we excised individual ubiquitylation bands and analyzed them via LC-MS/MS. The band positions were cut from lane 10 and indicated by the arrows in Fig 4.2. Table 4.1 shows the diGLY modified peptides identified in each sample which confirm that both AECR and AECR-N8 ubiquitylate histones. Interestingly, histones H3 and H4 were by far the most abundant identified proteins in each sample as they both appear in more than one sample each. The most abundant diGLY-modified peptides in sample 1 were identified as H3 and H4 respectively. Presence of these proteins correspond to the addition of Ub(8.5 kDa) to histone H4(19.5 kDa) in Figure 4.2. Sample 2 contained multiple diGLY-modified peptides corresponding to H3 which correspond to the addition of ubiquitin on H3(23.5 kDa) and the position of the band in Fig 4.2.

H2A diGLY-modified peptides were identified only in Sample 2 which may mean H2A is only mono-ubiquitylated. Sample 3 contained diGLY-modified peptides corresponding to both H4 and Ub. The presence of diGLY-modified ubiquitin in this sample suggests that H4 may be undergoing poly-ubiquitylation. Sample 5 contained multiple di-GLY modified peptides for H3 and Ub, suggesting again that H3 may be polyubiquitylated in this region. Sample 6 contained diGLY modified peptides for H3, H4 and Ub, and sample 7 contained diGLY modified peptides for H3 and Ub. Similar samples 3-5, these samples are likely poly-ubiquitylated H3 and H4. Interestingly, the most abundant peptides in every sample containing H3 identified diGLY modifications at K57. Such consistent results suggest that AECR is specific for H3K57 ubiquitylation. Similarly, H4K32 diGLY modifications appear with regularity in the samples which suggests AECR is also specific for H4K32 ubiquitylation. Ub peptides were also consistently modified at K48, indicating the presence of K48-linked poly-ubiquitylation which is known to signal for proteasomal degradation.

Table 3.1: List of diGLY modified peptides for AECR-N8 reaction gel samples. Listed below are diGLY modified peptides identified in the AECR-N8 reaction from Fig 3.2 and their corresponding sample, intensities, and diGLY sites.

Sample	Peptide	Modification Type	Protein	Intensity	Ascore	DiGLY site
1	R.YQK(+114.04)STELLIR.K	Ubiquitin	H3	1.71E+06	33.98	57
2	R.YQK(+114.04)STELLIR.K	Ubiquitin	H3	6.81E+08	1000	57
2	R.RYQK(+114.04)STELLIR.K	Ubiquitin	H3	1E+08	33.98	57
2	R.NDEELNK(+114.04)LLGR.V	Ubiquitin	H2A	1.22E+06	1000	96
3	R.DNIQGITK(+114.04)PAIR.R	Ubiquitin	H4	1.37E+07	17.01	32
3	R.LIFAGK(+114.04)QLEDGR.T	Ubiquitin	Ubiquitin	3.76E+07	1000	48
4	R.YQK(+114.04)STELLIR.K	Ubiquitin	H3	1.12E+09	1000	57
4	R.Y(+27.99)QK(+114.04)STELLIR.K	Ubiquitin	H3	2.61E+06	30.46	57
4	R.LIFAGK(+114.04)QLEDGR.T	Ubiquitin	Ubiquitin	1.87E+06	1000	48
5	R.RYQK(+114.04)STELLIR.K	Ubiquitin	H3	2.51E+05	23.10	57
5	R.YQK(+114.04)STELLIR.K	Ubiquitin	H3	3.56E+06	30.46	57
5	R.LIFAGK(+114.04)QLEDGR.T	Ubiquitin	Ubiquitin	6.49E+05	1000	48
5	I.FAGK(+114.04)QLEDGR.T	Ubiquitin	Ubiquitin	4.21E+07	1000	48
6	R.RYQK(+114.04)STELLIR.K	Ubiquitin	H3	2.68E+07	33.98	57
6	R.YQK(+114.04)STELLIR.K	Ubiquitin	H3	4.45E+08	33.98	57
6	R.DNIQGITK(+114.04)PAIR.R	Ubiquitin	H4	7.28E+06	33.98	32
6	I.FAGK(+114.04)QLEDGR.T	Ubiquitin	Ubiquitin	1.37E+06	1000	48
7	R.YQK(+114.04)STELLIR.K	Ubiquitin	H3	1.96E+08	26.02	57
7	R.RYQK(+114.04)STELLIR.K	Ubiquitin	H3	1.45E+07	1000	57
7	I.FAGK(+114.04)QLEDGR.T	Ubiquitin	Ubiquitin	1.27E+06	1000	48

2. AECR CUL5 K724R Mutant Retains Histone Ubiquitylation Activity

I conducted a similar ubiquitylation assay of histone octamers by AECR with wtCUL5 or CUL5 K724R. The CUL5 K724R mutant was generated to eliminate any chance of CUL5 ubiquitylation at K724. The mutation from a lysine to arginine prevents the attachment of Nedd8 or Ubiquitin which we expected to eliminate AECR's tendency to auto-ubiquitylate. Additionally, we suspected that ubiquitylation of K724 may cause a similar conformational change in AECR similar to neddylation, so we wanted to confirm that histone ubiquitylation is not dependent on any modification at CUL5 K724. Figure 4.3 shows an SDS-PAGE analysis with a similar layout to Fig 4.2 where lanes 1-4 indicate the relative positions of histone octamers and ubiquitylation machinery. Lanes 5-6 served as auto-ubiquitylation controls for AECR in the absence of histone octamers. By comparing lanes 5 and 6, it is evident from the band intensity and lack of higher bands that the CUL5 K724R mutant undergoes little to no auto-

ubiquitylation. Additionally, it appeared that ASB9 auto-ubiquitylation was greatly reduced in lane 6 by comparing the band intensities of ASB9 between lanes 5 and 6 and the lack of bands that appear in the 36-98 kDa range. These results confirm that auto-ubiquitylation activity is dependent on initial ubiquitylation of CUL5 K724. Lanes 8 and 9 contained ubiquitylation reactions of histone octamers by AECR with wtCUL5 and CUL5 K724R, respectively. An initial comparison between the two lanes showed much less banding in the CUL5 K724R sample which indicates there was less background auto-ubiquitylation activity. Despite the decreased presence of bands, there still were shared bands between the 16-36 kDa and 36-98 kDa ranges in both samples. Specifically, the bands indicated by the S1-4 markers in Fig. 4.3 are shared between both samples. These are the same bands we confirmed by LC-MS/MS to contain histones which confirms that AECR CUL5 K724R retains its histone ubiquitylation activity. The ubiquitylation bands in the AECR wtCUL5 reaction sample appeared slightly darker overall, but this could be due to the presence of auto-ubiquitylation activity.

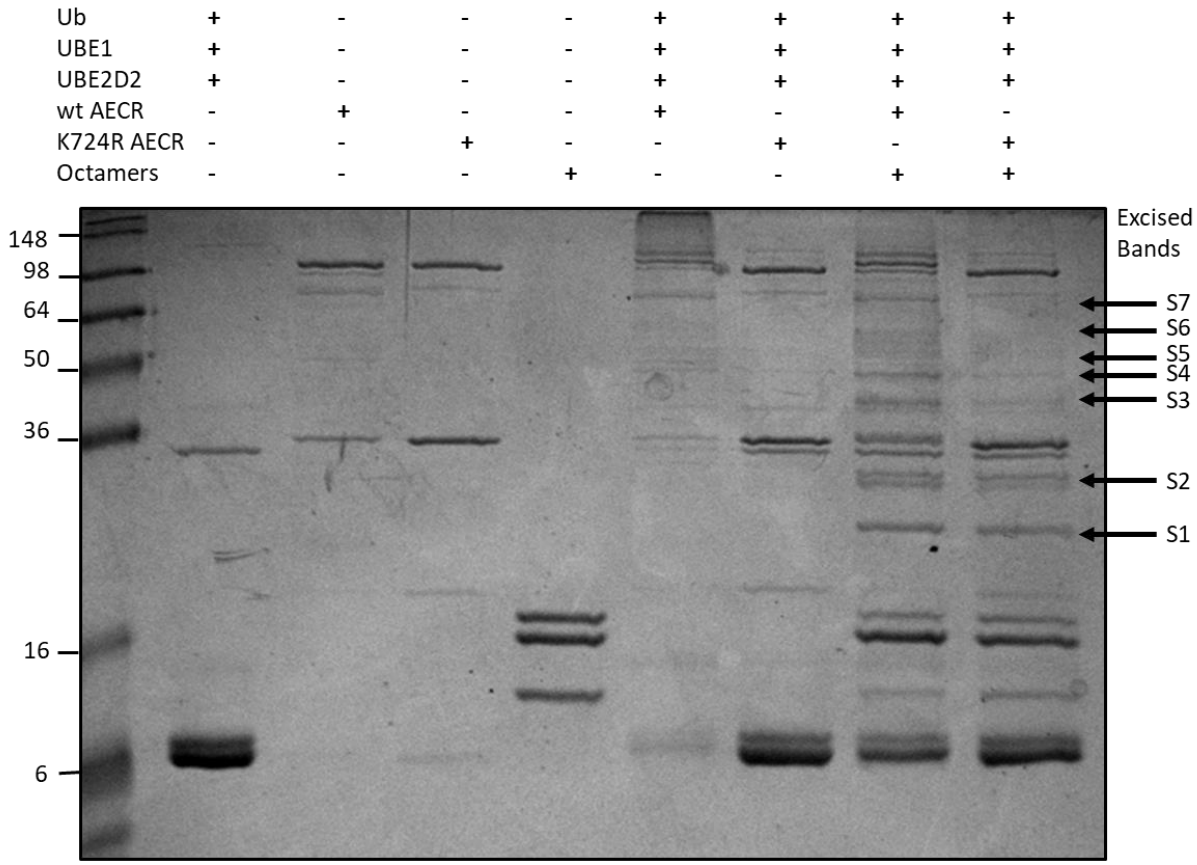

Figure 3.3: Ubiquitylation of Histone Octamers by AECR with wtCUL5 or CUL5 K724R. Lanes 2-5, References for each protein position; Lanes 6 & 7, Controls for auto-ubiquitylation of wtCUL5 or CUL5 K724R. Lanes 8 & 9, Ubiquitylation of *Xenopus* octamers by AECR with wtCUL5 or CUL5 K724R. Arrows indicate gel bands excised from lane 9 for Mass Spectrometry

To compare any differences in ubiquitylation activity between wild-type and the K724R mutant, I ran both reaction samples briefly onto an SDS-PAGE gel and excised the entire samples for MS/MS as described above. Overall, much less variety of diGLY identified peptides were detected compared to the individual gel band samples from the previous MS/MS experiment. This could be due to a higher amount and variety of protein within the gel bands in the reaction sample which could cause higher disparities between peptide intensities. Despite this, results were consistent with diGLY identifications from the previous MS/MS experiment, with H3K57, H4K32, UbK48 and UbK63 diGLY modified peptides identified. DiGLY modified peptides in the K724R reaction sample were almost identical to the wild-type sample, with

H3K57 H4K32 and UbK48 diGLY peptides identified. These results confirm that Histone octamer ubiquitylation by AECR is not dependent on CUL5 neddylation or ubiquitylation. The K724R mutant ubiquitylation activity confirms what I saw in the previous ubiquitylation experiment when I compared AECR-N8 and AECR ubiquitylation activity. The biggest difference in ubiquitylation patterns between wild-type AECR and K724R mutant is the absence of UbK63 diGLY peptides, which again could be due to intensity fluctuations.

To further confirm the activity and specificity of the K724R mutant, I excised seven bands from the gel in Fig 3.2 in the same positions as Fig 3.1 to compare the sample contents by LC-MS/MS. Table 3.2 contains the list of diGLY modified peptides identified in each reaction sample along with their intensities, protein identification and diGLY site. Compared to the results in Table 3.1, sample contents were almost identical overall, confirming that AECR specifically ubiquitylates H3K57 and H4K32 with or without neddylation or ubiquitylation at CUL5 K724. H3 diGLY peptides appeared less frequently than the previous set of samples which could be due to differences between gel excision or lower overall signal intensities. Interestingly, I saw presence of multiple K63Ub diGLY peptides which may indicate AECR is capable of both K48 and K63-linked poly-ubiquitylation. From these results, I can conclude that the K724R mutant does not auto-ubiquitylate and ubiquitylates histone substrates identically to wild-type AECR. Further, AECR appears to specifically ubiquitylate H3K57 and H4K32.

Table 3.2: List of diGLY modified peptides for AECR CUL5 K724R reaction gel samples.
Listed below are diGLY modified peptides from the AECR CUL5 K724R reaction sample in Fig 3.3 and their corresponding sample, intensities, and diGLY sites.

Sample	Peptide	Modification Type	Protein	Intensity	Ascore	DiGLY site
1	R.DNIQGITK(+114.04)PAIR.R	Ubiquitin	H4	1.84E+07	27.96	32
2	K.YQK(+114.04)STELLIR.K	Ubiquitin	H3	6.52E+07	26.02	57
2	R.NDEELNK(+114.04)LLGR.V	Ubiquitin	H2A	9.64E+04	1000	96
2	R.RYQK(+114.04)STELLIR.K	Ubiquitin	H3	1.26E+06	14.02	57
3	R.DNIQGITK(+114.04)PAIR.R	Ubiquitin	H4	4.78E+06	17.01	32
3	R.LIFAGK(+114.04)QLEDGR.T	Ubiquitin	Ubiquitin	3.45E+06	1000	48
4	R.LIFAGK(+114.04)QLEDGR.T	Ubiquitin	Ubiquitin	6.66E+06	1000	48
4	R.RYQK(+114.04)STELLIR.K	Ubiquitin	H3	8.37E+05	15.91	57
4	R.YQK(+114.04)STELLIR.K	Ubiquitin	H3	4.87E+07	30.46	57
5	R.LIFAGK(+114.04)QLEDGR.T	Ubiquitin	Ubiquitin	3.74E+06	1000	48
6	K.YQK(+114.04)STELLIR.K	Ubiquitin	H3	2.18E+06	27.46	57
6	R.DNIQGITK(+114.04)PAIR.R	Ubiquitin	H4	2.77E+06	24.44	32
6	R.LIFAGK(+114.04)QLEDGR.T	Ubiquitin	Ubiquitin	4.78E+06	1000	48
6	R.TLSDYNIQK(+114.04)ESTLHLVLR.L	Ubiquitin	Ubiquitin	1.40E+06	15.73	63
6	R.YQK(+114.04)STELLIR.K	Ubiquitin	H3	2.18E+06	27.96	57
7	R.DNIQGITK(+114.04)PAIR.R	Ubiquitin	H4	2.49E+06	26.02	32
7	R.LIFAGK(+114.04)QLEDGR.T	Ubiquitin	Ubiquitin	8.66E+06	1000	48
7	R.TLSDYNIQK(+114.04)ESTLHLVLR.L	Ubiquitin	Ubiquitin	5.10E+06	22.85	63
7	R.YQK(+114.04)STELLIR.K	Ubiquitin	H3	1.59E+06	27.96	57

D. Discussion

1. Specific H3 and H4 Ubiquitylation Could Involve Crosstalk with other Histone Modification Pathways

Through in vitro ubiquitylation assays and MS/MS mass spectrometry I identified that AECR preferentially ubiquitylates and histones H3 and H4 at lysines K57 and K32 respectively. Understanding the effects of histone modifications are an important part of deciphering the histone code. The effects of histone ubiquitylation are less understood compared to other PTMs, but histone ubiquitylation has so far been implicated mainly in proteasomal degradation and double-stranded DNA repair response. In these cases, histones are typically monoubiquitylated at the C-terminal tail and are shown to induce crosstalk with other PTMs like acetylation and methylation. For example, the polycomb repressive complex (PCR1) is known to monoubiquitylate H2AK119 and induce chromatin condensation by recruitment of histone methyltransferases (*9*). The little information on H3K56 and H4K32 ubiquitylation is limited to

proteomic identification of endogenous Ub sites (*8, 10*). Thus, there is *in vivo* evidence that H3K57 and H4K32 are ubiquitylated, yet no information on its biological significance. Examining a 3D structure of the nucleosome particle shows that H3K57 and H4K32 are located on the outer surface of the histone octamer, in proximity of the dsDNA backbone. I postulate that ubiquitylation at H3K57 and H4K32 could sterically inhibit chromatin condensation, preventing nucleosome formation.

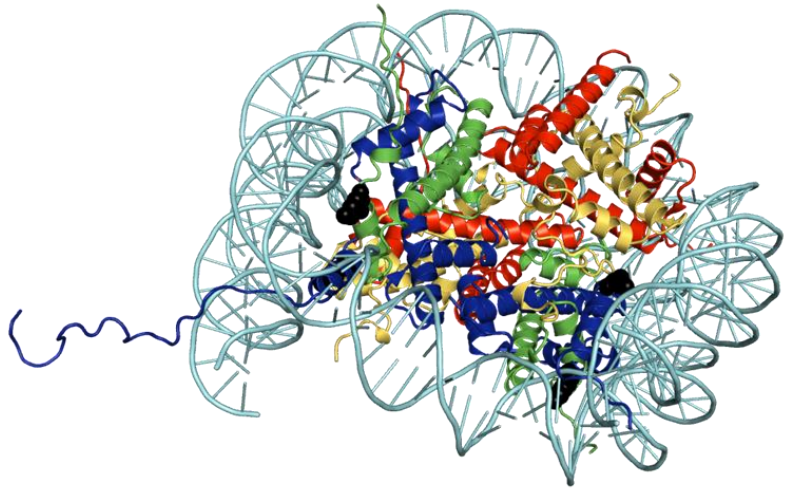

Figure 3.4: 3-D structure of *Xenopus laevis* nucleosome. (PDB ID: 1AOI). Gold: H2A, Red: H2B, Blue: H3, Green: H4. Black spheres indicate Lysines H3K57 and H4K32 which are specifically ubiquitylated by AECR.

2. Neddylation Activation is Not Required for ASB9-CUL5 Dependent Ubiquitylation of Histones

After screening the activities of wtAECR, AECR-N8 and AECR CUL5 K724R, I can confirm that Neddylation or Ubiquitylation of CUL5 does not affect histone ubiquitylation. This disagrees with the current-standing hypothesis that Neddylation of CRLs is required for activation. These results suggest Nedd8's role in ubiquitylation may be more nuanced than one would expect. Neddylation may have unique effects on ubiquitylation depending on the E3 enzyme, the substrate, or E2 enzyme. Substrate dependency would make sense given that Nedd8

influences conformational changes in Rbx2, potentially bringing the substrate in closer proximity to the E2-Ub conjugate. Such a conformational change could have more or less pronounced effects depending on the size or shape of the substrate. Neddylation of CRLs has also been shown to recruit other E3 ligases. For example, the RING-between RING (RBR) ligases Triad1 and HHARI are auto-inhibited for ubiquitylation on their own but display greatly increased activity when associated with neddylated CUL5 (*11*). Thus, neddylation may act as an extra mode of regulation for specific substrates that require other proteins to be recruited for proper ubiquitylation.

E. Conclusions

Here I characterize the histone octamers as a novel substrate AECR and AECR-N8 by *in vitro* activity assays, MS/MS identification and site-directed mutagenesis. Through these experiments I have identified that AECR does not require neddylation for ubiquitylation of the octamers, contrary to the current hypothesis that neddylation is required for CRL activity. Additionally, I identify that AECR specifically ubiquitylates histones H3K57 and H4K32, novel ubiquitylation sites that have been observed in *in vivo*, but whose biological pathway or modifying enzymes are unknown. Further biophysical study of histone binding to AECR would clarify the mechanism of ubiquitin transfer in this system

F. References

1. Debrincat, M. A., Zhang, J. G., Willson, T. A., Silke, J., Connolly, L. M., Simpson, R. J., Alexander, W. S., Nicola, N. A., Kile, B. T., and Hilton, D. J. (2007) Ankyrin repeat and suppressors of cytokine signaling box protein Asb-9 targets creatine kinase B for degradation, *J Biol Chem 282*, 4728–4737.

2. Balasubramaniam, D., Schiffer, J., Parnell, J., Mir, S. P., Amaro, R. E., and Komives, E. A. (2015) How the ankyrin and SOCS box protein, ASB9, binds to creatine kinase, *Biochemistry 54*, 1673-1680.

3. Schiffer, J. M., Malmstrom, R. D., Parnell, J., Ramirez-Sarmiento, C., Reyes, J., Amaro, R. E., and Komives, E. A. (2016) Model of the ankyrin and SOCS box protein, ASB9, E3 ligase reveals a mechanism for dynamic ubiquitin transfer, *Structure 24*, 1248-1256.

4. Andresen, C. A., Smedegaard, S., Sylvestersen, K. B., Svensson, C., Iglesias-Gato, D., Cazzamali, G., Nielsen, T. K., Nielsen, M. L., and Flores-Morales, A. (2014) Protein interaction screening for the ankyrin repeats and suppressor of cytokine signaling (SOCS) box (ASB) family identify Asb11 as a novel endoplasmic reticulum resident ubiquitin ligase, *J Biol Chem 289*, 2043-2054.

5. Shiyanov, P., Nag, A., and Raychaudhuri. (1999) Cullin 4A associates with the UV-damaged DNA-binding protein DDB., *J. Biol. Chem. 274*, 35309–35312.

6. Woodcock, C., and Dimitrov, S. (2001) Higher-order structure of chromatin and chromosomes., *Curr Opin Genet Dev 11*, 130–135.

7. Wang, H., Wang, L., Erdjument-Bromage, H., Vidal, M., Tempst, P., Jones, R. S., and Zhang, Y. (2004) Role of histone H2A ubiquitination in Polycomb silencing., *Nature. 431*, 873-878.

8. Kim, W., Bennett, E. J., Huttlin, E. L., Guo, A., Li, J., Possemato, A., Sowa, M. E., Rad, R., Rush, J., Comb, M. J., Harper, J. W., and Gygi, S. P. (2011) Systematic and quantitative assessment of the ubiquitin-modified proteome, *Mol Cell 44*, 325-340.

9. Endoh, M., Endo, T. A., Endoh, T., Fujimura, Y., Ohara, O., Toyoda, T., Otte, A. P., Okano, M., Brockdorff, N., Vidal, M., and Koseki, H. (2008) Polycomb group proteins Ring1A/B are functionally linked to the core transcriptional regulatory circuitry to maintain ES cell identity., *Development. 135*, 1513-1524.

10. Lumpkin, R. J., Gu, H., Zhu, Y., Leonard, M., Ahmad, A. S., K.R., C., Meyer, J. G., Bennett, E. J., and Komives, E. A. (2017) Site-specific identification and quantitation of endogenous SUMO modifications under native conditions., *Nat Commun 8*, 1171.

11. Kelsall, I. R., Duda, D. M., Olszewski, J. L., Hofmann, K., Knebel, A., Langevin, F., Wood, N., Wightman, M., Schulman, B. A., and Alpi, A. F. (2013) RIAD1 and HHARI bind to and are activated by distinct neddylated Cullin-RING ligase complexes., *EMBO J. 32*, 2848-2860.

Chapter IV

Biophysical Characterization of ASB9-Histone Interactions by Hydrogen-Deuterium Exchange Mass Spectrometry

A. Introduction

The Ankyrin repeat and Suppressor of Cytokine Signaling(SOCS) box(ASB) family of proteins are known to associate with and act as substrate receptors for Cullin-RING ligase (CRL) type ubiquitin ligases. ASB proteins are characterized by their N-terminal Ankyrin-repeat motifs and their C-terminal SOCS box. The Ankyrin repeat domain can be found throughout nature and is known to enable protein-protein interactions and binding events. Within the SOCS box there are two specific motifs called the Cullin box and BC box which interact with Cullin 5(CUL5) and Elongins B & C (EloBC) respectively to form the full ASB-EloBC-Cullin 5-Rbx2 (AECR) ligase complex. Additionally, CRLs are believed to be activated by the modification of CUL5 with the ubiquitin-like molecule Nedd8.

There is much to be understood about ASB proteins, namely their binding partners and relevant biological pathways. ASB9 is one of the more extensively studied proteins of the ASB family which was initially identified as binding partner for Brain-type Creatine Kinase (CKB) and were found to share similar levels of expression predominantly in the testes and kidneys. Additionally, they found that polyubiquitylation and proteasomal degradation of CKB occurs in an ASB9-dependent manner (1). CKB has been known to be overexpressed in tumors and may be used as a potential marker for metastasis, though it is unknown what factors induce ASB9 expression. Biophysical studies have shown that CKB binds as a dimer to ASB9 at the Ankyrin-repeat domain where the first Ankyrin repeat inserts itself between the cleft of the CKB monomers, inhibiting CKB activity (2,3). Since then, no other binding partners for ASB9 were identified until a proteomics study of the ASB family found that ASB9 binds to a diverse set of proteins. Among the identified proteins were known interacting partners like various types of

CK, but most notably the histone monomers H2A, H2B, H3 and H4 were all identified as interacting partners.

Histones form an octamer consisting of two H2A/H2B dimers and an H3/H4 tetramer. These octamers contain a high amount of lysines and arginines on their surface, making them highly positively charged. *In vivo*, dsDNA wraps around histone octamers at roughly 146bp per octamer, forming nucleosomes. Nucleosomes can further condense into higher-order structures like chromatin, and eventually chromosomes(4). Nucleosomes are subject to a variety of post-translational modifications (PTMs) that can alter the structure of chromatin by either tightening the interactions between DNA or loosening them. Nucleosomes undergo all types of PTMs, including ubiquitylation, which can induce signals in the cell such as chromatin condensation or DNA-damage response in addition to proteasomal degradation (5). Histones are also known to interact with proteins containing ankyrin repeat domains. My previous experiments recombinantly expressing and purifying AECR have shown AECR is capable of mono- and possibly polyubiquitylating *Xenopus laevis* histone octamers in an *in vitro* ubiquitylation assay. Further, my MS/MS experiments confirmed that AECR specifically ubiquitylates H3K57 and H4K32 in a Nedd8-independent fashion. Here, I further characterize the interactions between H3/H4 and the portion of AECR containing ASB9 and EloBC (AE).

B. Materials and Methods

1. Expression and Protein Purification of AE and H3-H4 Tetramer

Expression and purification of all proteins was identical to as described in Chapter 2 Methods.

2. HDX Experiments

HDXMS was performed using a Waters Synapt G2Si equipped with a nanoACQUITY UPLC system with H/DX technology and a LEAP autosampler. Individual proteins and

complexes were purified by size-exclusion chromatography (Superdex 200; GE Healthcare) in size-exclusion buffer(20mM Tris-HCl pH 8.0, 100mM NaCl, 1mM DTT, 5% Glycerol) prior to analysis. A sample of individual AE was concentrated to 5 µM while a sample of AE mixed with H3-H4 was concentrated at a 1:2 ratio to 5uM and 10uM, respectively. For each deuteration time, 4-µL of each sample was equilibrated to 25 ºC for 5 min and then mixed with 56 µL D_2O buffer [25 mM Tris (pH 7.5), 150 mM NaCl, 1 mM DTT, and 0.5 mM EDTA in D_2O] for 0, 0.5, 1, 2, or 5 min. The exchange was quenched with an equal volume of quench solution [3M guanidine and 0.1% formic acid (pH 2.66)].

The quenched sample was injected into the 50-µL sample loop, followed by digestion on an in-line pepsin column (immobilized pepsin, Pierce, Inc.) at 15 ºC. The resulting peptides were captured on a BEH C18 Vanguard pre-column, separated by analytical chromatography (Acquity UPLC BEH C18, 1.7 µM, 1.0 x 50 mm, Waters Corporation) using a 7-85% acetonitrile in 0.1% formic acid over 7.5 min, and electrosprayed into the Waters Synapt G2Si quadrupole time-of-flight mass spectrometer. The mass spectrometer was set to collect data in Mobility, ESI+ mode; mass acquisition range of 200-2000 (*m/z*); and scan time of 0.4 s. Continuous lock mass correction was accomplished with infusion of leu-enkephalin (*m/z* = 556.277) every 30 s (mass accuracy of 1 ppm for calibration standard). For peptide identification, the mass spectrometer was set to collect data in MS^E, ESI+ mode instead.

The peptides were identified from triplicate MS^E analyses of 5 µM AE and 5/10 µM AE/H3-H4, and data were analyzed using PLGS 3.5 (Waters Corporation). Peptide masses were identified using a minimum number of 250 ion counts for low energy peptides and 50 ion counts for their fragment ions. The peptides identified in PLGS were then analyzed in DynamX 3.0 (Waters Corporation). The following cut-offs were used to filter peptide sequence matches:

minimum products per amino acid of 0.2, minimum score of 6, maximum MH+ error of 3 ppm, a retention time standard deviation of 5%, and the peptides were present in two of the three ID runs. After back-exchange correction (30%), relative deuterium uptake for each peptide was calculated by comparing the centroids of the mass envelopes of deuterated samples with undeuterated controls. All experiments were performed in triplicate.

C. Results

1. HDXMS of AE with H3-H4 Tetramer

To characterize the binding interactions of AE with H3-H4 tetramer, I performed HDXMS experiments on free AE and AE bound to H3-H4 to identify any regions of AE that may bind to H3-H4. Specifically, we were looking for regions within the Ankyrin repeat domain of AE since it is known that CKB binds tightly to residues 25-42 within the first Ankyrin repeat region. Unexpectedly, the opposite effect was observed in AE where most of the ankyrin repeat domain experienced less protection in the bound state with H3-H4 than in the free state. Figure 4.1 shows the homology model of AE colored based on deuterium fractional uptake difference between the free and bound states. Blue corresponds to regions of AE that exchange more or exhibit no change when bound to H3-H4 than in the free state while red corresponds to regions of AE that show more protection when bound to H3-H4. A few peptides were selected to represent each type of exchange. Residues 25-42 of ASB9 which consist of the first half of the first ankyrin repeat and the disordered N-terminal region show much higher exchange upon binding of H3-H4. This trend of increased exchange continues throughout most of the Ankyrin repeat domain until the β-turn between Ankyrin repeats 4 and 5. Residues 43-59 continue to show increased exchange, albeit at a slower rate, while residues 64-140 show modest but significant increases in exchange. Interestingly, the region spanning residues 150-235 which

consist of half of ankyrin repeat 4 and ankyrin repeats 5 and 6 show very little difference uptake between open and closed states. Exchange again increases for the remainder of the protein.

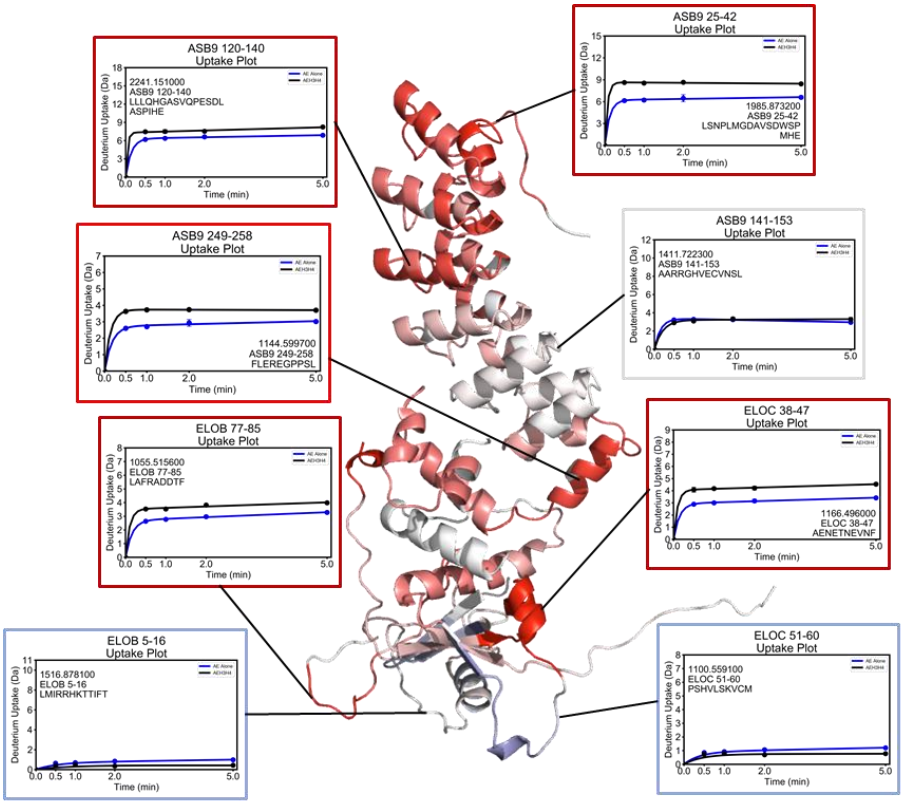

Figure 4.1: HDXMS of free AE versus AE bound to H3-H4. The fractional uptake difference of AE versus AE with H3-H4 was colored onto the homology of AE based on a red-white-blue color scale from -0.2 (blue) to 0.2 (red). Representative peptides are outlined based on their color on the structure.

Fractional uptake difference for EloBC show a wider range of results. On average, both EloBC display increased exchange throughout, but there are regions of protection observed. Elongin B residues 5-16 and Elongin C residues 47-61 show about 10% more protection. Interestingly, both protected regions of EloBC are in proximity of each other which may suggest either a binding event or an allosteric conformational change in this region.

D. Discussion

1.Different H3-H4 Binding Regions May Suggest a Unique Mechanism of Ubiquitin Transfer

Based on the fractional uptake difference of AE bound H3-H4 versus free AE, it is evident that AE becomes more dynamic in the presence of H3-H4. The first four Ankyrin repeats of ASB9 increase in exchange by 10 percent or more which suggests the H3-H4 tetramer does not bind in this region. This is a notable result as previous studies have shown that CKB binds tightly to the first Ankyrin repeat region of ASB9 and increases protection in this region (2). Interestingly, the regions between Ankyrin repeats four and six do not show increased exchange which suggests this region remains less dynamic during binding and could be due to potential H3-H4 tetramer interactions. Additionally, modest protection of EloB residues 5-16 and EloC residues 46-60 are also observed which could suggest binding or some type of conformational change in this region. Regardless, the presence of the H3-H4 tetramer seems to induce allosteric changes within most of ASB9 and EloBC, resulting in increased dynamic movement throughout the complex.

Figure 4.2 illustrates the full structure of AECR, consisting of CUL5, Rbx2 and Nedd8. AE retains its fractional uptake difference color scheme to show areas of exchange. UbE2D2-Ub is positioned above Rbx2 to illustrate its relative position during ubiquitin transfer. A histone octamer or tetramer bound to either region of AE may be closer in proximity to the E2-Ub than if positioned near the first Ankyrin repeat. The increased dynamic movement of AE could bring the histone substrate close enough to the E2-Ub to complete ubiquitin transfer. Additionally, if the histone substrate does bind to either region during ubiquitin transfer, either unique binding position may explain why AECR does not require neddylation to ubiquitylate the histone substrate. Neddylation induces conformational changes in Rbx2 and CUL5 C-terminal domain such that ubiquitin transfer is in closer proximity if a substrate such as CKB binds to the first Ankyrin repeat of ASB9, and unneddylated AECR shows little to no ubiquitylation of CKB.

Thus, histone substrate binding in either observed protected region could be close enough such that neddylation is not required for ubiquitin transfer.

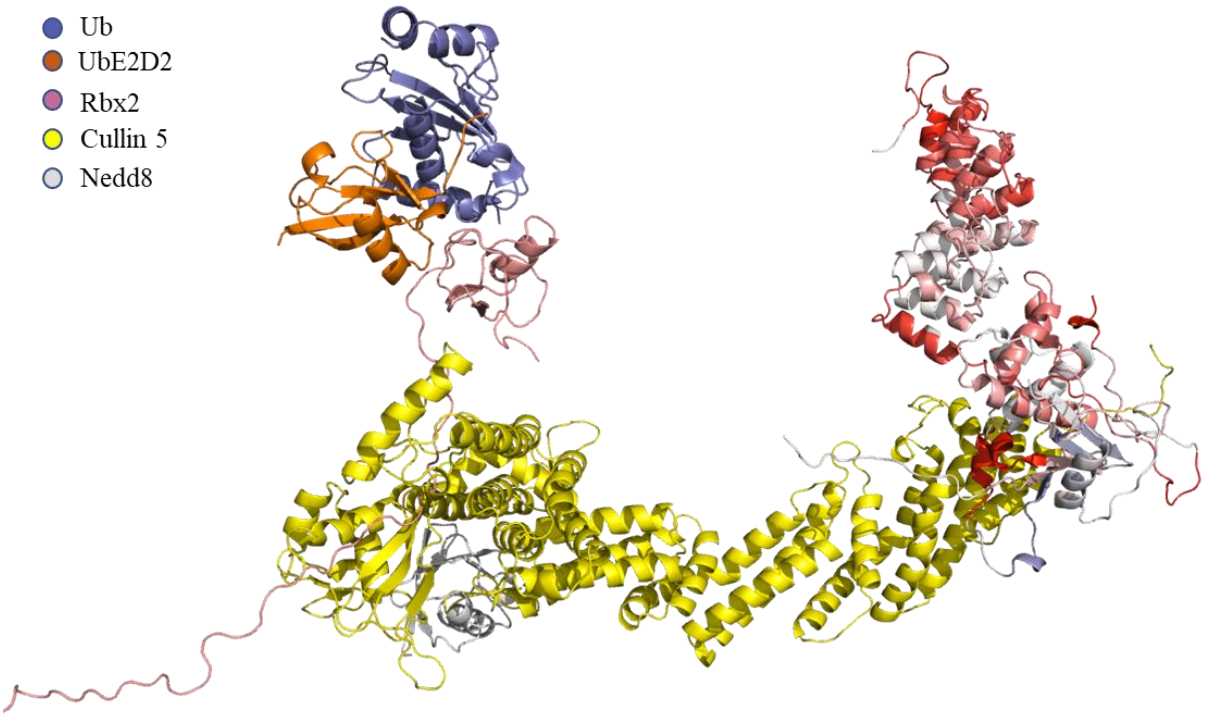

Figure 4.2: Homology Model of the AECR-N8 Structure. The full ligase structure of AECR-N8 was assembled from crystal structures using SWISS model homology modeling software. Proteins are colored according to the legend in the top-left corner. AE is colored based on its fractional uptake difference identical to Fig. 4.1.

E. Conclusions

Here I characterize the binding interactions between AE and the H3-H4 tetramer through HDXMS experiments. Unexpectedly, tetramer binding increases dynamics in almost all regions of AE except two regions within ankyrin repeats 5-6 of ASB9 and near the N-terminus of EloB. These two unaffected regions suggest that the H3-H4 tetramer may bind to either region of AE, resulting in allosteric increases in dynamics of AE. The H3-H4 tetramer's potential binding sites, combined with AE's increased dynamics may bring it in closer proximity to the E2-Ub molecule when assembled as a full complex. These observations could suggest a novel mechanism of

ubiquitin transfer that does not require neddylation of CUL5. Further biophysical experiments such as study of octamer or nucleosome binding may better characterize this novel mechanism of ubiquitin transfer.

F. References

1. Debrincat, M. A., Zhang, J. G., Willson, T. A., Silke, J., Connolly, L. M., Simpson, R. J., Alexander, W. S., Nicola, N. A., Kile, B. T., and Hilton, D. J. (2007) *J Biol Chem* **282**, 4728–4737

2. Balasubramaniam, D., Schiffer, J., Parnell, J., Mir, S. P., Amaro, R. E., and Komives, E. A. (2015) *Biochemistry* **54**, 1673-1680

3. Schiffer, J. M., Malmstrom, R. D., Parnell, J., Ramirez-Sarmiento, C., Reyes, J., Amaro, R. E., and Komives, E. A. (2016) *Structure* **24**, 1248-1256

4. Woodcock, C., and Dimitrov, S. (2001) *Curr Opin Genet Dev* **11**, 130–135

5. Wang, H., Wang, L., Erdjument-Bromage, H., Vidal, M., Tempst, P., Jones, R. S., and Zhang, Y. (2004) *Nature.* **431**, 873-878